Distribution Agreement

In presenting this thesis or dissertation as a partial fulfillment of the requirements for an advanced degree from Emory University, I hereby grant to Emory University and its agents the non-exclusive license to archive, make accessible, and display my thesis or dissertation in whole or in part in all forms of media, now or hereafter known, including display on the world wide web. I understand that I may select some access restrictions as part of the online submission of this thesis or dissertation. I retain all ownership rights to the copyright of the thesis or dissertation. I also retain the right to use in future works (such as articles or books) all or part of this thesis or dissertation.

_____

Patrick S. Coppock

Single- and Double-Component Atomistic Models of Phosphatidylcholine Lipid Bilayers in the Gel and Liquid Crystalline Phases

By

Patrick S. Coppock

Doctor of Philosophy

Department of Chemistry

_____

Dr. James T. Kindt
Advisor

_____

Dr. Joel M. Bowman
Committee Member

_____

Dr. Michael C. Heaven
Committee Member

Accepted:

_____

Lisa A. Tedesco, Ph.D.
Dean of the Graduate School

_____

Date

Single- and Double-Component Atomistic Models of Phosphatidylcholine Lipid Bilayers in the Gel and Liquid Crystalline Phases

By

Patrick S. Coppock
M.S., University of South Florida, 2003

Advisor: James T. Kindt, Ph.D.

An Abstract of
A dissertation submitted to the Faculty of the
James T. Laney School of Graduate School of Emory University
in partial fulfillment of the requirements for the degree of
Doctor of Philosophy
in Chemistry
2010

Abstract

By Patrick S. Coppock

Atomistic computational models of molecular systems hold great promise in that (1) they are capable of giving high-resolution insight, (2) they are comparatively inexpensive, (3) they are highly adjustable, (4) they are basically waste-free, and (5) validation thereof with experimental reference points is trivial. In the last few decades, computational approaches to aggregate systems such as lipid bilayers have come of age. The increase in processor speeds coupled with the power of parallelization and the development of elegant methods has brought into range simulations of systems as large as hundreds of thousands of atoms and timescales into the microsecond regime. With these capabilities, it is increasingly important to develop and qualify good models. This dissertation is divided into three parts, all of which serve to evaluate and refine an atomistic model of phosphatidylcholine lipid bilayers in the gel and/or liquid crystalline (LC) phase.

In the first part, di-stearoyl-phosphatidylcholine (DSPC, di-C18-PC) and di-myristoyl-phosphatidylcholine (DMPC, di-C14-PC) in the gel and LC phases were simulated in the semi-grand canonical ensemble ($\Delta\mu PT$) at a temperature between their experimental main phase transition temperatures $T_{m,exp}$. Matched pairs ($x_{\mathrm{DSPC,gel}} : x_{\mathrm{DSPC,LC}}$) were identified that were in good agreement with experimental systems, and demixing was observed in the gel phase, where strong deviations from ideality were manifested by a tendency for the short-tail lipid to laterally associate. In the second part of this thesis, a two-phase (gel and LC) system was simulated with a pre-existing interface to probe the phase character over a range of temperatures. DSPC and di-palmitoyl-phosphatidylcholine (DPPC, di-C16-PC) were simulated in the isothermal-isobaric ensemble (NPT) at temperatures far below and above the supposed T_m. Both melting and congealing was observed, and fitting the rates of transition to an Arrhenius-like equation gave estimates of $T_{m,virtual}$ within about 5 K, or a 2 % error in terms of absolute temperature. Investigation of congealing interfaces revealed that, while tails of lipids deposited onto an existing gel adopt the same tilt angle and direction as the host gel, the glycerol backbones are arranged in a disordered pattern, even if the backbones of the host gel are aligned. This glycerol-backbone orientational disorder has been observed experimentally and is the focus of the next section. Finally, two gel models were described and compared. Except the gel model introduced in the first part of this thesis, all gel models described in the literature have been based on the crystal structure. Here, two gels are described and compared, one with disorder in the glycerol-backbone super-lattice, and the other aligned and oriented, like the crystal structure. The backbone-disordered gel is shown to be more like experimental gels structurally and thermodynamically. The structures of gels are shown to be highly influenced by the initial configuration, and the significant effect of backbone arrangement on the overall structure suggests that models of the gel phase should not be based on the crystal structure without regard to defects in the backbone super-lattice.

Single- and Double-Component Atomistic Models of Phosphatidylcholine Lipid Bilayers in the Gel and Liquid Crystalline Phases

By

Patrick S. Coppock
M.S., University of South Florida, 2003

Advisor: James T. Kindt, Ph.D.

A dissertation submitted to the Faculty of the
James T. Laney School of Graduate School of Emory University
in partial fulfillment of the requirements for the degree of
Doctor of Philosophy
in Chemistry
2010

Acknowledgments

First, I thank the National Science Foundation, the Camille and Henry Dreyfus Foundation for financial support, and American citizens for prioritizing science.

I thank my advisor, Professor James T. Kindt. Jill and I started planning for this stage of my training about 2 years before I started. I spent a lot of time on the Internet reading about scientists that were doing work that appealed to me, and Dr. Kindt's group was an early favorite. After reading and corresponding with a few scientists, I came to Emory, specifically to work with him. I came with high hopes, and I have not been disappointed. I say without hesitation that Dr. Kindt has exceeded my hopes in virtually every aspect. He is an exemplary scientist, a brilliant teacher, and a superb manager. He is strong in my areas of weakness, and in my areas of strength, he seems to be stronger. Most of my praise I shall leave in general terms, but two things I want to say explicitly: (1) I have known people who are good at correcting without seeming to correct, but I do not think I have ever seen anyone do it as artfully as James. He can unambiguously tell you that you are wrong, how so, and then leave you feeling as if he never noticed. And (2) he is a master of understanding what is in your head, and then addressing a problem from your vantage point. I have a brother who is the world's best at that, and James just may be better. Thank you, James. May gracious and competent people surround you, and may they aid you as you have aided others.

I thank the members of my dissertation committee, Professors Joel Bowman and Michael Heaven. It is very gratifying to have scientists of your stature on my committee. Though I have spent many an uncomfortable moment taking questions from my committee, I feel like your questions have given me a far greater appreciation for nuance, and by extension, the gestalt of Physical Chemistry. Thank you for your efforts on my behalf.

I thank my teachers; Alex Kaledin, Joel Bowman, Michael Heaven, Tim Lian, James Kindt, and Fereydoon Family. When I was visiting Emory in the spring of 2006, I sat in Dr. Bowman's office. With his calm and engaging manner, he folded his hands on the table, and said, "Now Patrick, you should know that we are going to 'get under the hood,' so to speak. We are going to get our hands dirty." I was thrilled. And I have been thrilled to sit in your classes. I have been amazed---truly amazed---at your clarity of thought, at your cogent presentations. Physical Chemistry is full of wonders, and I appreciate that you are in a position to understand them, and to show them to me. Finally, I thank you for giving homework assignments and grading them line-by-line. Your specific feedback, though often painful (probably for both of us), has been a key factor in my progress. I also thank my science teachers from previous periods of training, Gary Parker, Leon Mandell, David Bedell, and Tom Lamb.

Over the years, I have been blessed with classmates that have unselfishly aided me in my studies. Right or wrong, my feelings of gratitude scale with the degree to which I was in need. The material that I have undertaken for this stage of my training was far and away the most challenging of anything I have ever attempted. Thus, my thankfulness to my current classmates and colleagues---accurately expressed---would certainly seem

superfluous. Therefore I will simply say to Chantelle Anfuso, Teddy Huang, Ivan Antonov, Keith Freel, Marcia Gomes, Fuchang Yin, among others, thank you. Thank you so much.

I am thankful to my parents for many things. Most pertinent to this current work, I thank them for asking a lot of questions and parsing concepts a lot in my presence as a child. I also thank them for telling me I was bright---I think they believed it---and showing me how to aspire even in the face of difficulty.

I am thankful to Jill, my dulcet wife. It would be impossible for me to exaggerate the strength and grace you bring to our home. You and I, and *only* you and I, know the extent to which this period of my training is a gift from you to me. Like the other gifts you have given me, my doctoral training has been (1) a great thrill, (2) of great long-term value, and (3) very costly to you. Thank you.

Finally, I am thankful to the God of the Bible, and His Son, Jesus Christ, Maker and Sustainer of all.

O LORD, our Lord,
How majestic is Your name in all the earth,
Who have displayed Your splendor above the heavens!
From the mouth of infants and nursing babes You have established strength
Because of Your adversaries,
To make the enemy and the revengeful cease.
When I consider Your heavens, the work of Your fingers,
The moon and the stars, which You have ordained;
What is man that You take thought of him,
And the son of man that You care for him?
Yet You have made him a little lower than God,
And You crown him with glory and majesty!
You make him to rule over the works of Your hands;
You have put all things under his feet,
All sheep and oxen,
And also the beasts of the field,
The birds of the heavens and the fish of the sea,
Whatever passes through the paths of the seas.
O LORD, our Lord,
How majestic is Your name in all the earth!

Table of Contents

List of Tables

List of Figures

References to Previously Published Work

Chapter 2 appears in its entirety as

> "Atomistic Simulations of Mixed-Lipid Bilayers in Gel and Fluid Phases", Patrick S. Coppock and James T. Kindt, *Langmuir*, **2009**, 25(1), 352-359.

Chapter 3 appears in its entirety as

> "Determination of Phase Transition Temperatures of Atomistic Model Lipid Bilayers from Stripe Domain Growth Kinetics", Patrick S. Coppock and James T. Kindt, *Journal of Physical Chemistry B*, accepted, **2010**.

1 Introduction

1.1 Overview

The importance of the cell membrane has long been understood, but the last few decades have shed a great deal of light on the complexity, not just of the membrane, but also of the life-supporting processes occur on or within it. Modern understanding of membranes hinges on the concept of heterogeneity, the idea that the membrane is organized in domains with different compositions and functions,(1-3) rather than mixed randomly as in an "ideal" mixture at equilibrium. As domains are also formed associated with phase transitions even in relatively simple one-, two-, and three-component bilayers, study of the phase character of lipid bilayers, first single component systems and then mixtures, has been recognized as central to understanding membrane phenomena.

Theoretical models of lipid bilayers have made important contributions to this effort,(4, 5) but computational models, because of their expense particularly at atomistic resolution, are much less mature. The first simulations of lipid bilayers were reported over 30 years ago,(6, 7) but atomistic simulations extending into the nanosecond regime have only been reported in the last 15 years.(8) Aspects of molecular systems that can be sampled in the picosecond regime include bulk densities, density profiles and conformational dynamics. Rotational and translational diffusion of lipids takes hundreds of nanoseconds to microseconds,(9-11) and phase transformations take anywhere from

hundreds of nanoseconds to days,(12-15) so the selection of a model and method depends largely on the phenomenon of interest.

"Coarse-grained" models, where groups of atoms are simulated as one particle are used to study systems with thousands of lipids and over time intervals into the microsecond regime. Nevertheless, they lack resolution, and can be hindered by significant blind spots.(16) I have used atomistic models for the sake of resolution and accuracy, and have employed various strategies to overcome the time constraints. For example, to investigate mixing statistics in a two-component system, I have used a semi-grand canonical ensemble with a constant difference in chemical potential $\Delta\mu = \mu_A - \mu_B$, where component *A* can be mutated to *B* or vice-versa based on a Monte Carlo move. I have addressed rate limitations of phase transitions by isolating the fast stage, phase propagation. I constructed a two-phase system with a pre-existing interface and monitored phase propagation (in either direction) over a range of temperatures. Finally, as simulation methods were unable to equilibrate slow rotational degrees of freedom in the lipid bilayer gel phase, I relied on modeling initial gel structures with different degrees of orientational order and choosing the one in best agreement with a range of experimental results. Two different approaches to molecular simulations are molecular dynamics and Monte Carlo (MC) simulations.

1.2 Molecular Dynamics

Classical Molecular dynamics (MD) simulations calculate trajectories of atomic or molecular systems comprised of N = hundreds to hundreds of thousands of particles. MD

simulations can be applied to extended systems by incorporating periodic boundary conditions (pbc) in 1, 2, or 3 dimensions. A trajectory is determined by solving Newton's equations of motions for *N* particles.

$$F_i = m_i \frac{d^2 r_i}{dt^2}, \text{ where}$$

$$F_i = \frac{-dU}{dr_i}.$$

where *U* is a function that gives the potential energy of the system as a function of all particle coordinates r_i. All simulations described in this dissertation were performed with the simulation package GROMACS.(17-19) The group of potential functions together with parameters are often collectively referred to as a force-field. The force-field used in all the simulations described in this dissertation was developed by Berger et al.(20) The potential is of the form

$$U = \sum U_{bond} + \sum U_{angle} + \sum U_{dihedral,prop} + \sum U_{dihedral,improp} + \sum U_{non-bonded}$$

This force-field is not flexible enough to describe the breaking or forming of chemical bonds, but is intended to capture molecular conformations and intermolecular interactions that control the structure and dynamics of a non-covalent aggregate such as a lipid bilayer.

1.3 Monte-Carlo Methods

Monte Carlo (MC) simulations of atomistic systems vary widely. Perhaps the most straightforward is the Metropolis algorithm,(21) which is based on the following algorithm:

(1) A particle is chosen at random.

(2) A new position is chosen for the particle by

$$x' = x + \text{rand}\left(\frac{-\Delta x_{\max}}{2}, \frac{\Delta x_{\max}}{2}\right)$$

(3) The new position is accepted according to the probability

$$p_{acc} = \min[1, \exp(-\beta \Delta U)]$$

Other approaches include volume or pressure "moves" or exchange of particles with a virtual reservoir.(22) Dynamical simulations of systems with many intermolecular degrees of freedom can be inefficient; random moves frequently result in highly improbable configurations. One way this has been addressed is with configurational-bias Monte Carlo (CBMC).(23) Briefly, CBMC samples configurations based on a bias, and then accepts them with a probability that assures they obey a Boltzmann distribution.

1.4 Monte-Carlo/ Molecular Dynamics Hybrid

A mixed MC-MD method was developed by our group(11, 24) and is the main method used in the first study(25) (described in chapter 2), as well as a supplement to the third study (described in chapter 4). It intercalates the MD steps with CBMD steps, where a short-tailed lipid (di-C14-PC) is switched with a long-tailed lipid (di-C18-PC), or *vice-versa*, based on the difference in their respective chemical potentials μ. It thus samples a constant $N_{tot}\Delta\mu PT$ ensemble, or semi-grand canonical ensemble. Given diffusion constants on the order of 10^{-8} $cm^2 \cdot s^{-1}$, the time for two lipids to switch place is about 200 ns. To assure equilibrium lateral distributions would take about 10 times that, which makes diffusive mixing prohibitively slow.

The remainder of this dissertation is organized as follows.

1.5 Thesis Outline

In **chapter 2**, we describe the phase coexistance of a two-component phosphatidylcholine system. Di-stearoyl-phosphatidylcholine (DSPC) and di-myristoyl-phosphatidylcholine (DMPC) differ in tail length by 4 methylene carbons. The experimental main phase transition temperature T_m, so called because it is reversible and observed without regard to system history, is 328 K for DSPC and 297 K for DMPC. We investigated DSPC/DMPC mixtures in the gel and liquid crystalline (LC) phases at 313 K at the same difference in chemical potential $\Delta\mu = \mu_{DSPC} - \mu_{DMPC}$, and found mixtures in both phases that were at least metastable on the simulation timescale (nanoseconds). From these, we were able to identify matched pairs of gel and LC structures whose compositions

($x_{DSPC,gel}$:$x_{DSPC,LC}$) were in qualitative agreement with experiment. The lateral distribution of lipids within each phase is very challenging to observe experimentally; the simulations showed random mixing within the LC phase, but significant clustering of the DMPC lipids within the gel.

In the process of this study, we observed a gel → LC phase transition when a critical threshold of the low melting point lipid (DMPC) was exceeded. The LC → gel congealing phase transition was never observed in this study. Congealing is a slower process, but the absence of this transition left us wondering if 313 K is between the T_m's of the model. I.e., if the force-field gives a $T_{m,DSPC}$ off by more than 5% in terms of absolute temperature, it could be lower than 313 K, which would mean that the gel-phase mixture studied at 313 K would not be stable no matter how low the DMPC content.

The extremely slow dynamics of phase transitions prevent simple comparison of T_m of a simulation model with experiment, which could be a useful validation tool for lipid force-fields. The LC → gel transition occurs in 4 stages, beginning with the nucleation of a gel domain within the LC. The creation of an interface has a high energy penalty, and is thus slow at temperatures close to the T_m, where the free energetic driving force for conversion of one phase into the other vanishes. **Chapter 3** describes our approach to determining T_m in light of this challenge. We constructed a two-phase system with a pre-equilibrated gel "stripe" flanked on both sides with a pre-equilibrated LC. This system was simulated for 100 ns over a wide range of temperatures to observe the conversion of one phase to another at the pre-existing interface. The rates of transition were fit to a temperature-

dependent Arrhenius equation to estimate (1) a transition temperature, or the temperature at which the rate of phase transition is zero, and (2) an activation energy, to give insight into the molecular process(es) key to the transition. The dynamics of phase propagation were furthermore in agreement with experimental estimates within a factor of 2. This method was used for two different lipids, DSPC (di-C18-PC) and di-palmitoyl-phosphatidylcholine (DPPC, or di-C16-PC). Both lipid systems yielded transition temperatures $T_{m,virtual}$ that differed from experiment by about 5 K, or about a 2% error in terms of absolute temperature, a significantly smaller error than has been estimated using other simulation approaches.(26, 27)

Characterization of the phase interface in the gel-LC "stripe" simulations revealed a laterally disordered arrangement of the backbones of newly congealed lipids. The gel used in the two-phase model was based on the DMPC crystal structure, which is highly ordered in the glycerol-backbone super-lattice. Experiments have suggested this order is lost in the subgel → gel transition, and though the tails are arranged in a hexagonal lattice, the glycerol backbones are neither aligned nor orientationally ordered. **Chapter 4** compares two gel models, one with backbone disorder and the other ordered in the backbone super-lattice. Tail structure and glycerol-backbone order were considered, as well as their miscibility with DMPC, and the results for each model were compared with experiment. The two gels were similar in several respects, but in some respects the disordered structure was in significantly better agreement with experiment. These results highlight a feature of lipid bilayer gels that has been neglected in previously published simulation studies.

2 Atomistic Simulations of Mixed-Lipid Bilayers in the Gel and Fluid Phases

2.1 Introduction

Phase coexistence phenomena in multicomponent lipid bilayers have been studied for decades(1-3) but recently have attracted renewed interest as lipid domain or "raft" formation is increasingly thought to play a functional role in critical cellular processes.(4-8). In pure bilayers composed of phosphatidylcholine (PC) lipids with saturated alkyl tails, the L_β or "gel" and L_α or "liquid crystal" (LC) phases are the most important at full hydration. Although intermediate phases such as the sub-gel and ripple phases have also been observed, the transition between the gel and the LC is commonly called the main phase transition because its enthalpy of transition is orders of magnitude greater than the others, and because it is the only transition in fully hydrated bilayers that is reproducible without regard to system history.(9) The gel phase of a saturated PC lipid is similar to the solid, crystalline phase in that the acyl tail-groups are uniformly tilted with respect to the bilayer normal, packed in a hexagonal array, and predominantly in the extended all-*trans* conformation. The primary difference is that in the gel phase the headgroups and associated waters are generally disordered. The gel and LC phases differ mainly in the packing and order of the tails. In general, the gel acyl tails pack in a hexagonal lattice and at a tilt with respect to the bilayer normal. The LC lacks regular packing and has a higher fraction of tail dihedrals in the gauche conformation.

In pure bilayers, gel and LC domains may coexist only at a characteristic transition temperature T_m. In a binary mixture of lipids, gel-LC coexistence is typically possible over a range of temperatures. As a simple model for domains, bilayers formed from a mixture of the glycerophospholipids distearoylphosphatidylcholine (DSPC) and dimyristoylphosphatidylcholine (DMPC) have received a great deal of attention. DSPC has 18 carbons in each tail and an experimental T_m of 328 K, while DMPC has 14 carbons in each tail and an experimental T_m of 297 K.(3) Above the T_m of both lipids, they are fully miscible in a homogeneous LC phase. Between the transition temperatures of its components, a DMPC-DSPC mixture may exist in one of three states. If the DSPC content is below a lower coexistence composition threshold, it will dissolve in the DMPC to form a single homogeneous LC mixture. If the DSPC content is above an upper coexistence composition threshold, the DMPC will dissolve in DSPC gel to form a single homogeneous gel phase. Between these compositions, the system will consist of an inhomogeneous mixture of coexisting LC and gel sections; the fraction of the system that is LC or gel will depend on the total system composition while the phase compositions are fixed at the coexistence thresholds as required by the Gibbs phase rule. The upper and lower coexistence compositions both approach pure DSPC at the upper temperature; at the transition temperature of DMPC, the situation is complicated by the possibility of gel-gel coexistence, which will not be addressed here.

The DMPC/DSPC mixture has been modeled using a range of techniques. Simple lattice models, paramaterized to fit experimental observables such as the T_m of the pure components, are able to address structural properties such as size distributions/geometrical properties of clusters and to calculate various thermodynamic properties.(10-13) Stevens used a coarse-grained (CG) model to simulate the formation of ordered domains of long-tailed lipids in a binary mixture, and the trans-bilayer correlation of these domains.(14) Another CG simulation shows the beginning of the liquid-gel phase transition starting with nucleation of 20-80 lipids within tens of nanoseconds, while pockets of disorder persist into the microsecond regime.(15) Faller and Marrink used a CG model to investigate domain formation in mixed bilayers and to simulate LC to gel phase transitions, successfully reproducing details of the phase diagram.(16) These approaches have yielded useful insights into the physics underlying the phase behavior and the structural properties of mixed-lipid systems at the lengthscale of domains but are limited in ability to provide molecular-scale structural insight.

Few molecular simulation studies of the gel phase have been conducted using atomistic models. In 1996, Tu et al. performed a 20 ps molecular dynamics (MD) simulation on DPPC. They found good agreement with experimental measurements of density profiles and other structural properties such as area per lipid.(17) Venable et al. simulated the DPPC gel for up to 4.5 ns in 2000. Among other results, they found that (1) flexible cell geometry was necessary, and (2) Ewald summations of electrostatics were superior to spherical cutoffs.(18) In 2002, acyl tail packing and conformation were described for both the gel and the liquid crystal in a comparison of simulation results with IR

spectroscopic data.(19) de Vries et al. incubated 256 well-hydrated DPPC lipids at 283 K, well below the main transition temperature, to yield a ripple phase that contains some gel-like character; they also report (in supplemental material) the formation of gel phases from 300 ns simulations at this temperature.(20) Most recently, Leekumjorn and Sum reported simulations of heating and cooling bilayers past their expected transition temperatures that demonstrate a loop of hysteresis, where the physical characteristics such as area per lipid evolve from LC-like values to gel-like values, but in a manner that depended on the system history.(21) A reversible order-disorder transition is apparently too slow to observe on the time scale of 10^{-8} to 10^{-7} seconds that is commonly accessed in atomistic MD simulations. In a binary mixture, equilibration of a phase-separated mixture is slowed further by the need for demixing via lateral diffusion of the two components between domains. With lateral diffusion constants of $\sim 8 \times 10^{-8}$ $cm^2 \cdot s^{-1}$ in the LC phase,(22) the mean time required for a lipid to diffuse 5 nm is about 1 μs; diffusion within a gel is yet slower.

In the present study, DSPC/DMPC mixtures in the gel and LC phases are simulated with atomistic detail using a mixed Monte Carlo-Molecular Dynamics (MC-MD) method designed to eliminate the need for diffusion in simulations of lipid mixtures.(23) With this method, after each molecular dynamics step, an attempt is made to mutate a randomly selected lipid in the bilayer from DSPC to DMPC or *vice-versa*. Appropriate acceptance criteria are used to maintain the system within a semi-grand canonical ensemble, i.e., at a fixed difference $\Delta\mu$ between the two components' chemical potentials and at thermal equilibrium. The MC-MD technique has previously been applied to

DPPC/DLPC mixed bilayers in the fluid phase(23) and to investigate demixing of lipids at bilayer edge defects and regions of different curvature.(24) Here, it is applied to characterize the lateral and normal distributions of the two lipids in a mixed gel phase. The dependence of composition on Δm offers insight into the thermodynamic non-ideality of DMPC/DSPC mixing within gel and LC phases. Knowledge of Δm also provides some insight into the conditions necessary for these phases to coexist, although by itself this information is insufficient to calculate equilibrium phase boundaries.

2.2 Methods

2.2.1 *Construction of the DSPC Gel*

The initial configuration of the gel structure was constructed with Spartan (Wavefunction, Inc.) according to the crystal structure published by Pearson and Pascher for DMPC.(25) The unit cell of the crystal structure has 4 lipids in it, with 2 unique lipids in each leaflet and one water of hydration per lipid. The crystal structure was used as a template; since the gel does not have static waters of hydration, the waters from the crystal structure were ignored. The energy of the molecules was minimized for about 1000 steps using MMFF in Spartan.(26-29) The minimized structure was converted to a (4 molecule) bilayer and expanded by replicating the structure once along each in-plane axis using utilities provided with GROMACS 3.2,(30) making a 16-lipid bilayer with an area per lipid of 0.482 nm^2. 400 Single point charge (SPC) waters(31) were added to this structure using the GROMACS genbox utility and it was minimized (steepest descents, 100 steps). The structure was replicated again in each of the in-plane axes. The resulting

64-lipid configuration was equilibrated using the united-atom force-field described by Berger(32) for 8 ns at 313 K, giving an area per lipid of 0.481 nm^2. A 32-lipid section was taken from this structure and the hydration level adjusted to 25 waters per lipid in a box with dimensions 3.20 nm × 3.20 nm. Three vacancies on each leaflet were created in transferring the 32-lipid section to the smaller box. During a further 10 ns MD equilibration, rearrangements were observed in the structure, including the azimuthal direction of the tail tilt angles changing from an $L_{\beta F}$ structure to an $L_{\beta I}$ structure(33) and the re-establishment of a defect-free hexagonal array of tails. During the closing of vacancies, a disruption of the ordered molecular packing occurred. Three of the 32 lipids were rotated out of alignment, such that the displacement vector between their tails formed a 60˚ angle with respect to the other lipids. Three more of the 32 lipids adopted wide-stance conformations in which their two tails occupied next-nearest neighbor positions in the hexagonal array of tails. The structure at the end of this equilibration, with dimensions 2.82 nm × 2.82 nm, was again doubled in both in-plane axes to make a 128-lipid system, and equilibrated via MD for 50 ns. This final MD trajectory did not lead to qualitative changes to the lipid packing, with about 24 lipids remaining in non-standard orientations.

2.2.2 Construction of DSPC Liquid Crystal

A previously equilibrated DPPC liquid crystal(23) was used to create the DSPC LC phase by separating two leaflets by 1.3 nm and adding two carbons per tail. After a brief minimization with GROMACS (100 steps of steepest descent), the system was

equilibrated for 20 ns using MD as described. The number of waters per lipid was adjusted to 25. The system was equilibrated for 50 ns at 313 K and 333 K, and parameters otherwise as described above for the gel. Measurements of all three constructs, the gel at 313 K and the two LCs, were averaged over the last 10 ns. Table 1 compares these parameters with some notable experimental results.

For all MD calculations, the Berendsen barostat(34) was used with semi-isotropic pressure coupling, with a time constant of 2 ps, a compressibility of 4.5×10^{-5} $bars^{-1}$ and a reference pressure of 1 bar. The Langevin thermostat(35) was used with a time constant of 0.2 ps. Electrostatic forces were calculated by particle mesh Ewald[36] and a timestep of 2 fs was used.

2.2.3 *Monte Carlo-Molecular Dynamics*

A Monte Carlo-Molecular Dynamics hybrid simulation code, used previously in a study of DPPC-DLPC mixtures in the fluid phase,(23) was used with identical parameters in the present study. To summarize briefly, every MD step is followed by a Monte Carlo (MC) move attempt, in which one lipid is chosen at random for a trial mutation move. If the lipid is the long-tailed lipid (DSPC in this case), a successful move removes the last four united-atom carbon sites on each tail, while if it is the short-tailed lipid, a successful move extends both tails by four sites. Positions for the new sites in a DMPC→DSPC move and acceptance probabilities for both types of MC moves are generated using the

configuration-bias MC algorithm developed by Siepmann et al.(36, 37) with 4 trial positions generated for each chain tail segment. The acceptance probabilities for all DSPC→DMPC moves (and DMPC→DSPC moves) were weighted by the standard activity ratio α (or its inverse α^{-1}):

$$\alpha \equiv a_{DMPC} / a_{DSPC} = \exp(\beta \Delta\mu) \quad (1)$$

where a represents the thermodynamic activity of a component, $\beta = (k_B T)^{-1}$, and $\Delta\mu = \mu_{DMPC} - \mu_{DSPC}$. Typical success rates were 1 in 1000 for LC phase simulations and 1 in 500 for gel phase simulations.

MC-MD simulation was performed using the equilibrated 128-DSPC gel or LC structures as an initial configuration for 25 ns over a range of activity ratios. Analysis of mean composition, radial distribution functions, and site density profiles was carried out on the last 10 ns of each run.

2.3 Results and Discussion

2.3.1 *Pure Bilayer Structures*

Fig. 1 shows that key structural properties for all three configurations stabilized within three nanoseconds during the initial equilibration, although the area per lipid of the gel phase continued a slow drift upwards over at least the first 30 ns. The evolution of area per lipid and the fraction of acyl tail dihedrals in the *anti* (i.e. trans) geometry are given

for a pure DSPC gel phase at 313 K and two pure DSPC LC phases, one at 313 K and the other at 333 K. The observed stability over the simulation timescale of both phases at 313 K reflects the slowness of phase transitions---one phase or the other is in a metastable state. In previously published simulations, complete gel-to-LC transitions have only been observed over trajectories of several hundreds of nanoseconds(21) As the experimental transition temperature for DSPC is 328 K, we expect that the DSPC LC phase is in the metastable state at this temperature. On the other hand, we cannot assume that the model reproduces the experimental T_c: an estimate from the literature places the transition temperature of DPPC, modeled using the same force-field parameters, at 10 K lower than the experimental transition.(21) The area per lipid values obtained for both phases are in reasonable agreement with experiment, as shown in Table 1. The fraction of *trans* and *gauche* dihedrals in the gel phase varies strongly with position along the acyl tail, with lowest values in the middle of the chain, in qualitative agreement with previous simulation results.(19) Bonds 5-10 are all close to 2.5% *gauche*, in good agreement with the experimental value of 2.3 ±1.1% obtained by IR for the 6-position of the gel phase of DPPC at 311 K.(38)

Table 2.1 *Comparison of Structural Parameters of pure DSPC bilayers with Experimental Values*

System	Area/ Lipid (nm^2)	Tilt (degrees from normal)	Method	Reference
Gel, 313 K	0.502	37.5	MD	current work
Gel, 298 K	0.473	33.5	X-ray	(39)
Gel, 293 K	0.520	38	X-ray	(40)
LC, 313 K	0.628	-	MD	current work
LC, 333 K	0.658	-	MD	current work
LC, 338 K	0.660	-	^{2}H NMR	(41)
LC, 353 K	0.701	-	^{2}H NMR	(41)

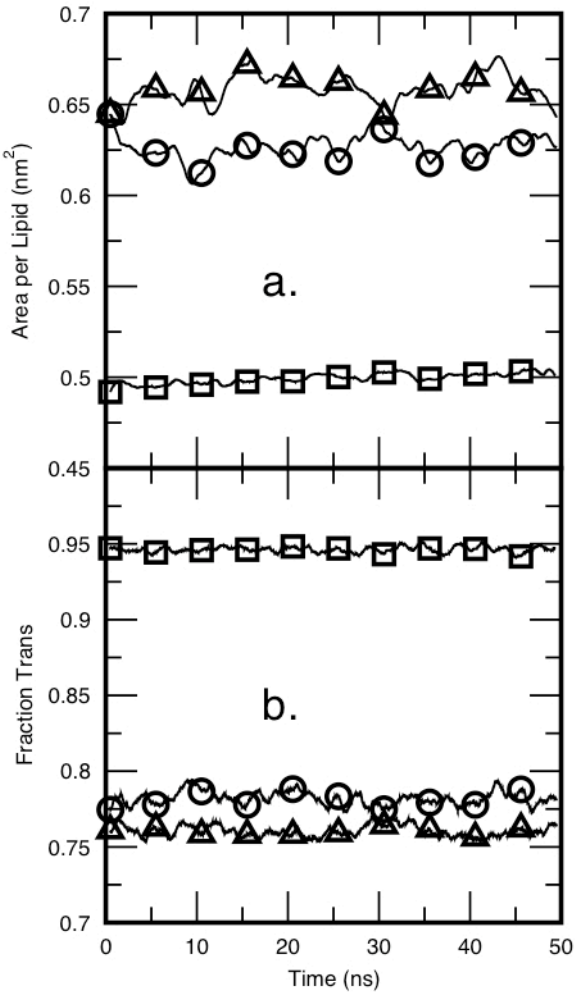

Figure 1. Panel a.; *Area per Lipid vs. Time.* Areas per lipid of three pure DSPC bilayer constructs are shown, the LC at 333 K (triangles) and at 313 K (circles), and the gel at 313 K (squares). Panel b.; *Fraction of Acyl Tail Dihedrals in Anti- Conformation vs. Time.* Fractions of the tail anti- dihedrals for the constructs, LC at 333 K (triangles) and 313 K (circles) and gel at 313 K (squares). The curves in both panels represent running averages over 1 ns.

For reference during the analysis of lateral distribution of DMPC/DSPC mixtures, the 2-dimensional radial distribution functions (rdf's) were calculated from the lateral (in-plane) distances between centers of mass of lipids belonging to the same leaflet in pure DSPC bilayers (see fig. 2). As seen in a previous atomistic PC gel simulation a sharp

nearest-neighbor peak at 0.5 nm is followed by a broader feature that appears to encompass multiple peaks.(17) The first peak integrates to two nearest neighbors and the second to four, a distribution consistent with a distorted hexagonal lattice. The center of mass (COM) radial distribution for individual tails (not shown), in contrast, is consistent with local hexagonal packing, with six nearest neighbors in the first peak. These two arrangements are easy to reconcile. The individual tails are able to pack as independent molecules. Looking down the primary axis of the tails reveals they occupy a space that is basically cylindrical, and thus pack in a hexagonal lattice. On the other hand, the lipid center is located between the two tails; i.e., the footprint of each lipid is oblong, resulting in distorted hexagonal packing. The radial distribution of the 64-lipid $L_{\beta F}$ gel precursor structure, whose molecular packing is more ordered (see Methods), is shown for comparison. The presence of a minor peak at 0.8 nm in the radial distribution of the 128-lipid structure but not the 64-lipid structure suggests that this peak correlates to lipids whose glycerol backbone alignment differs their neighbors'. Since the lateral distributions were calculated as a function of the lipid centers of mass, the radial positions at the defect sites in the 128-lipid gel are affected by the orientation relative to neighboring lipids. The rdf of the LC phase, which is comparatively featureless, reflects the lack of regular order.

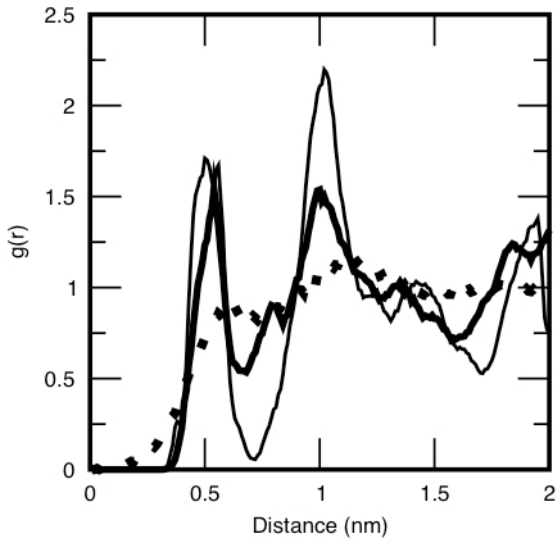

Figure 2. *Lateral Radial Distribution of Lipids in Pure DSPC Bilayers.* Distributions of lateral distances were calculated from lipid centers of mass, including only pairs of lipids within the same leaflet, for the 64-lipid gel system (see Methods) (thin, solid curve), 128-lipid gel phase with glycerol backbone disorder (heavy, solid curve) and LC phase (hashed curve).

2.3.2 *Semi-Grand Canonical Simulations of DSPC/DMPC Mixtures*

MC-MD simulations were performed over a range of activity ratios; equilibrated DSPC bilayers (gel and LC) were used as the starting configurations. In principle, systems should converge to the same state regardless of the starting configuration, except for a narrow window where the activity ratio matches that of a pair of phases that coexist at equilibrium. However, the rate of transition between gel and LC phases is slow on the nanosecond timescale, so significant hysteresis is observed (i.e., the starting phase in most cases determined the phase for the entire simulation), and there is significant overlap between the activity ratios at which gel and LC phases are kinetically stable.

Fig. 3 shows the dependence of mean composition (expressed as mole ratio) on activity ratio for gel and LC mixtures. In an ideal mixture, activity ratio is proportional to mole ratio, yielding a slope of 1 on the log-log plot as shown in the reference line. In the gel phase, ideal (or "ideal-dilute") behavior is seen for mixtures that are very dilute in DMPC, but a strong departure from ideal behavior is seen starting with a 1:10 DMPC-DSPC mole ratio and above. The sub-linear increase of activity ratio with mole ratio indicates a positive excess free energy of mixing, as one would expect for a mixture whose components ultimately undergo phase separation and partition unevenly into separate phases. In the LC phase, a more modest deviation from the ideal mixing curve appears close to 1:1 mixing ratio, as has been seen in similar mixtures in previous MC-MD simulations.(23, 24)

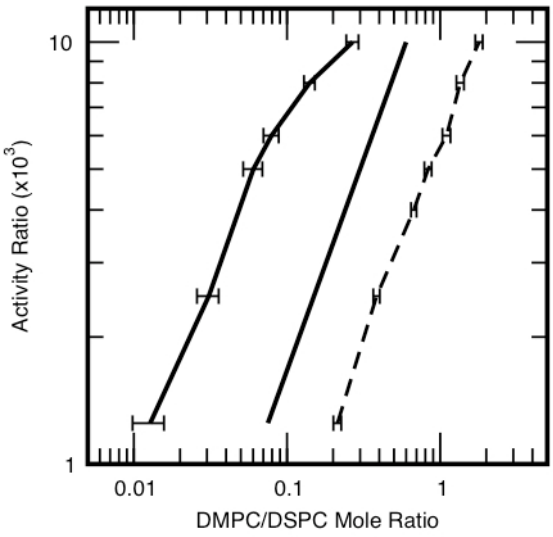

Figure 3. *Log-log plot of activity ratio (a_{DMPC}/a_{DSPC}) vs. average mole ratio for gel (solid curve at left) and LC (hashed curve at right) phases from MC-MD simulations.* For reference, a solid line representing a linear relationship between activity ratio and mole ratio is plotted between the curves.

A positive excess free energy of mixing—that is, a thermodynamic penalty associated with mixing two components, which counteracts the inherent entropic favorability of mixing—will in general be associated with an enhanced (relative to purely random mixing) tendency for the minority component to form pairs or clusters. Radial distribution functions for the lipid components, calculated using distances between centers of mass projected onto the plane of the bilayer, are shown in fig. 4. In the gel phase, there is a significant enhancement in the value of g(r) for the DMPC-DMPC pairs relative to the DSPC-DMPC pairs. The snapshots in fig. 5 illustrate what the clustering or lack thereof looks like at the end of the simulation. The greatest enhancement is seen in the shoulders at 0.8 nm and 1.3 nm. As discussed above in the section describing results for pure DSPC bilayers, these shoulders arise from defect sites in which the glycerol backbone has a different orientation about the bilayer normal than the majority of lipids in the gel; such sites appear to be especially prone to clustering. In the LC phase, no exceptional trend is seen in comparing the pair contributions to g(r) for like and unlike components.

To make the statistical distributions more concrete, we show the integrated mean excess of like neighbors as a function of distance (fig. 6). In a random mixture, the mean composition of all neighboring lipids in a sufficiently large circle drawn around a lipid of either type will be the same and will reflect the bulk composition. (This may not be true at short distances, as molecular sizes or shapes may lead to different distributions of neighbor distances for different types of neighbor, even if the overall distribution is random.) The excess like-neighbor function for a given lipid type (e.g. DMPC) is

obtained by first calculating the total number of DMPC lipid neighbors whose center of mass lies within a lateral distance *r* of the average DMPC lipid. Then the mean total number of all lipid neighbors within a lateral distance *r* of the average DMPC lipid is determined and multiplied by the average mole fraction of DMPC to yield the expected

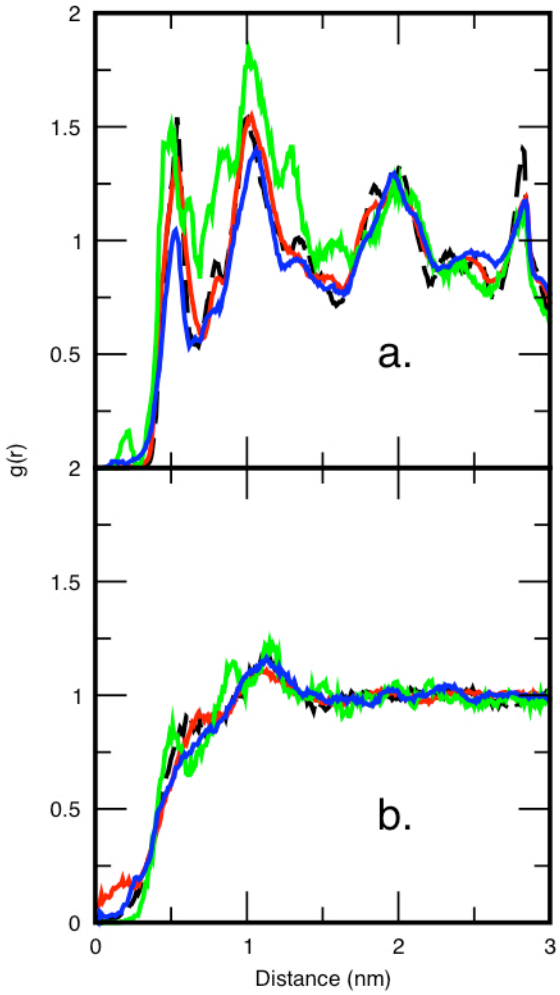

Figure 4. *Lateral Radial Distribution Functions in DMPC/DSPC bilayers from MC-MD simulations.* Gel phase 21:79 DMPC:DSPC bilayer (panel a) and 29:71 DMPC:DSPC LC phase bilayer (panel b). Distribution functions are calculated from in-plane distances between pairs of lipid centers of mass in the same leaflet. Pair distributions for DSPC-DSPC are represented in red, for DMPC-DMPC in green, and for DSPC-DMPC in blue. For comparison, results from single-component DSPC bilayers are shown as black, hashed curves.

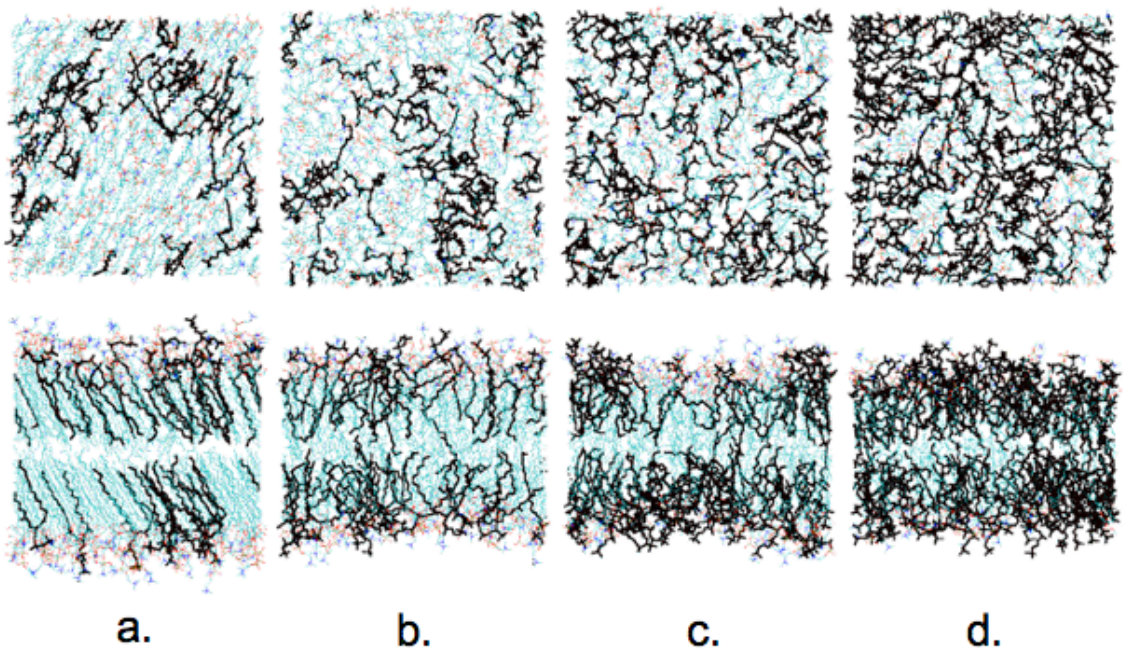

Figure 5. *Top view (upper row) and cross-sectional view (lower row) snapshots of final lipid structures after MC-MD simulation.* DMPC is indicated in black, DSPC is in lighter color. Pictured in column a. is the gel with a DMPC mole fraction of 0.21. Columns b.-d. are snapshots of LCs with mole fractions of 0.29, 0.52 and 0.64, respectively. Images created with VMD.(43)

number of DMPC neighbors for a random mixture. Around any lipid, the expected number of neighboring like lipids can be calculated as a function of distance. The excess number of like neighbors is defined as the difference between the actual number of neighbors of the same type and the expected number. A positive excess number reflects an effective attraction between like neighbors; the excess will be close to zero if the components are mixed randomly. In the gel, there is an excess of 0.8 DMPC neighbors above the random mixing prediction within the first hexagonal neighbor shell (1.0 nm) of the average DMPC, representing a 66% excess over the average of 1.2 DMPC neighbors predicted for a random mixture. The excess number of like neighbors for DSPC is smaller, as clustering of the minority component has relatively smaller effect on the

majority component. Though the interleaflet interactions are largely different than those within a leaflet, we also portray the excess number of like "neighbors" on the opposite leaflet in panels C and D. In the gel phase, there is again an excess of like lipids that may indicate a tendency for DMPC lipids to attract each other across the leaflets. Its significance is less obvious than that of the intra-layer correlation however, as the excess is only evident at greater distances, where the total integrated number of lipids is much greater (about 14 lipid neighbors at 15 nm), and the excess is proportionally smaller. As in previous work on DPPC/DLPC mixtures,(23) no significant positive or negative correlations in neighbor composition are apparent either within or across the leaflet in the fluid phase simulations. Experimental determination of the lateral distribution of lipids at the molecular level is quite challenging. According to a theoretical estimate based on mapping thermodynamic nonideality parameters obtained through analysis of the experimental phase diagram, the tendency of DMPC to pair with other DMPC in a 20% DMPC/80% DSPC mixed gel was estimated to be about a factor of 2 higher than would be expected from a random mixture, (44) in qualitative agreement with the present simulation results. However, that same method also yielded a 50% excess over random mixing for DMPC-DMPC pairing in fluid phase DMPC/DSPC mixed bilayers, which contrasts with the finding of essentially random mixing in the present simulations.

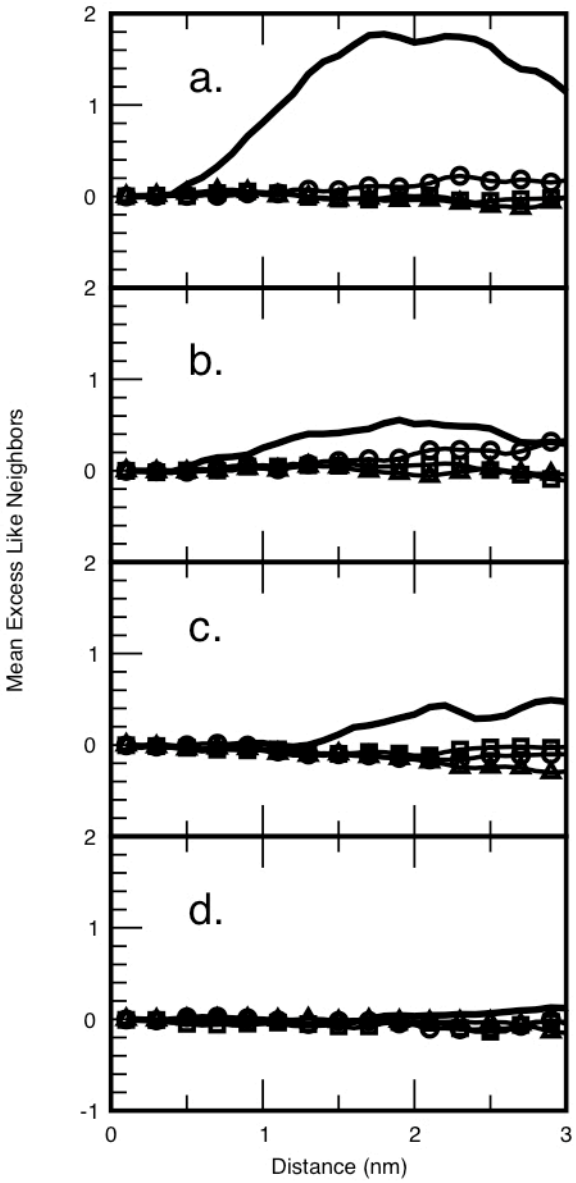

Figure 6. *Mean Excess Number of Like Neighbors vs. Lateral Radius of DMPC/DSPC Mixtures.* Mean excess like neighbor number functions were calculated as described in the text from MC-MD simulation data. Panel a. shows the intra-layer mean excess for DMPC, b. shows the intra-layer excess for DSPC, c. the trans-layer excess for DMPC, and d. the trans-layer excess for DSPC of like-neighbors. Gel phase results (mean DMPC mole fraction 0.21) are shown as solid curves in all panels, and curves outlined by squares, circles, and triangles depict LC phase data corresponding to average DMPC mole fractions 0.29, 0.52, and 0.64, respectively.

The tail length mismatch seems to be accommodated differently in the gel phase than in the LC, as indicated in distributions of the two components' sites along the bilayer normal (fig. 7). In the gel phase snapshot of figure 1, the headgroups of many of the DMPC lipids appear to be closer to the bilayer midplane than those of DSPC. The density profiles of the phosphorus and tail terminal methyl sites of DMPC and DSPC (fig. 7, panel b) confirm that on average, the headgroup phosphorus atoms of DMPC are shifted 0.1-0.2 nm towards the bilayer normal. This shift is not enough, however, for the tail end methyl groups of DMPC to reach as deep into the bilayer center as the DSPC. As the DMPC positioning appears to minimize both mismatches at once subject to the constraints of the molecular size difference, we can infer that mismatches in both headgroup and tail positions are energetically unfavorable in the gel. (The neighbor pairing of DMPC lipids in the gel phase, indicated in fig. 5 and fig. 6, reduces the number of DMPC/DSPC contacts, and therefore the amount of the mismatch penalty.) For the LC, the lipid headgroup phosphorus distributions do not shift along the bilayer normal axis, and the mismatch is entirely relieved by the methylene and methyl carbons at the ends of the DSPC tails (panels c. and d.). The disorder and fluidity of the tail end region in the LC phase, we can therefore infer, yields a tail mismatch penalty that is negligible compared with the headgroup penalty. The absence of a significant penalty for DMPC/DSPC contacts is consistent with the absence of a tendency towards neighbor pairing in the LC phase observed in fig. 5 and fig.6. In fact, in the low DSPC fraction system (panel d.), the distributions of DSPC methyl groups from the two leaflets are nearly superimposable, indicating that the long tails of these lipids extend partially into the opposite leaflet. As discussed in an MC-MD study of DPPC-DLPC LC mixtures,(23)

the ends of the DSPC tails from both leaflets tend to intermingle at the bilayer midplane, but in a disordered structure rather than any regular interdigitation. Like the site distribution profiles, trends in order parameters in the LC phase mixtures (shown in Supplemental material, figure 2) are qualitatively similar to those seen for DPPC-DLPC mixtures, with the order of both components decreasing with increasing short-tail component fraction. The gel phase shows no such commingling, as evident from the low degree of overlap of terminal methyl group distributions in figure 7b as well as the clear separation of leaflets in the gel structure snapshot of figure 5.

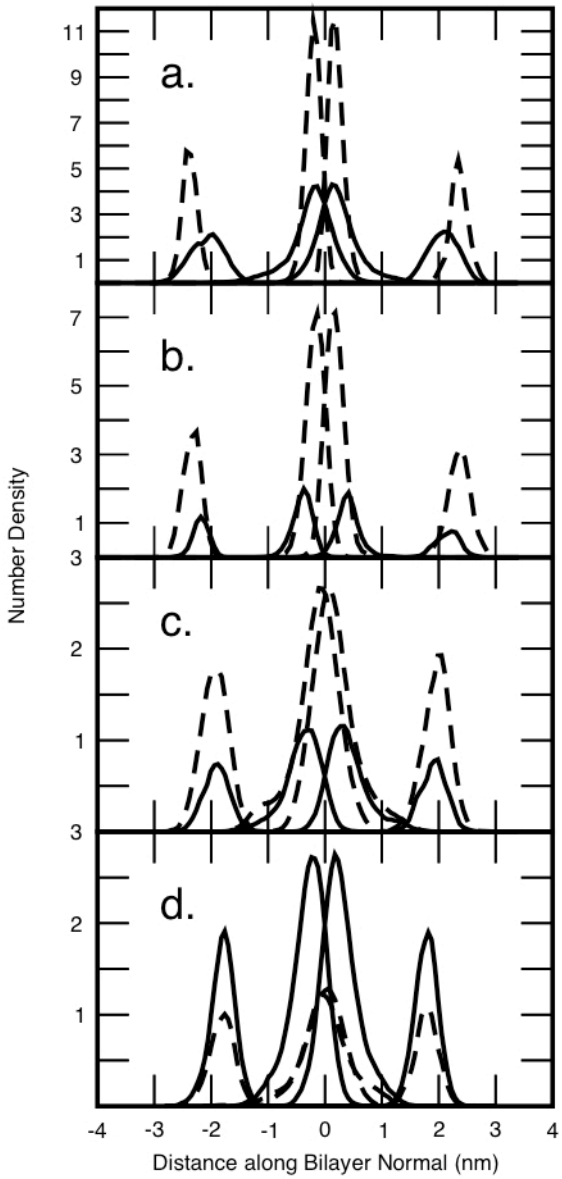

Figure 7. *Number density profiles of headgroups and terminal tail methyl-groups along bilayer normal.* Panel a. depicts the number distribution of the pure DSPC gel (hashed curve) and the pure DSPC LC (solid curve). Panels b.-d. show the number distributions of short-tailed lipids (DMPC) as a solid curve and those of the long-tailed lipid (DSPC) as a hashed curve. Panel b. is from a gel with a mean DMPC mole fraction of 0.21 and panels c. and d. are from LCs with mean DMPC mole fractions of 0.29 and 0.64, respectively.

For a pair of two-component phases to coexist at equilibrium, the chemical potential μ of each component in one phase must equal the chemical potential of the same component in the other phase. Semi-grand canonical ensemble simulation yields the composition of each phase as a function of activity ratio α (see eq. 1 and fig. 3). Two phases having the same activity ratio indicates they have the same difference in their components' chemical potentials, a necessary but not sufficient condition for stable phase coexistence, as illustrated graphically in figure 8. For each activity ratio α, we obtain two compositions---one for the gel phase and one for the LC---which represent a *possible* pair of coexisting phase compositions for the present model system and temperature. We might call the relationship between these phases a *semi-equilibrium*, because the phases are at equilibrium with respect to the exchange of lipids of different types but not necessarily with respect to the growth in number of lipids of one phase at the expense of the other. Our ability to evaluate which phase is more stable at a given activity ratio---and therefore to identify the pair of compositions corresponding to true equilibrium coexistence---is limited by the slow rate of transitions between the phases on our simulation timescale. Up to an activity ratio of $\alpha = 1.0 \times 10^4$, we see both phases stable over the course of the simulation, as shown in fig. 9. At a slightly higher activity ratio of $\alpha = 1.2 \times 10^4$ or above, in simulations initiated with a gel phase structure the DMPC content jumps (see fig. 9) along with area per lipid and tail disorder (data not shown) to values typical of the LC phase at this activity ratio. As "semi-equilibrium" cannot be established, the true equilibrium phase coexistence for our model must lie at lower activity ratios, and therefore at lower DMPC contents of both phases. We take the DMPC contents of the gel and LC phase at the highest activity ratio for which both phases are stable---21% and

64% DMPC respectively---as upper bounds to the compositions at equilibrium coexistence. Since we do not observe an LC-to-gel transition on the simulation timescale at this temperature even for 100% DSPC (as discussed above and demonstrated in Figure 2) we could not determine a corresponding lower bound to the DMPC content at coexistence.

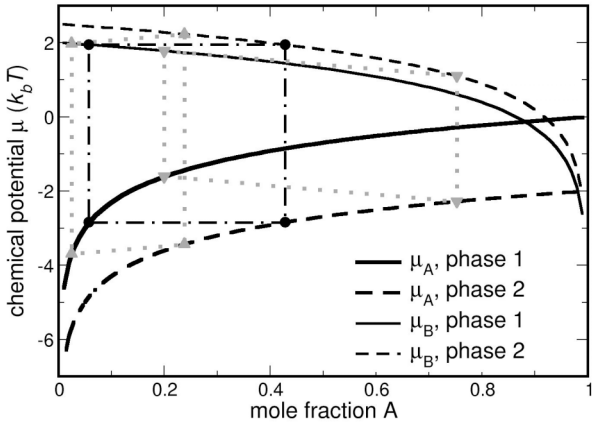

Figure 8. *Illustration of semi-equilibrium vs. equilibrium phase coexistence*. Chemical potential vs. composition is plotted for a hypothetical 2-phase, 2-component system. Solid black circles connected by dot-dash lines mark the true phase coexistence condition: matching of both components' chemical potentials across the phases occurs at a unique pair of compositions---in this case, at 5.8% A and 42.8% A for phase 1 and phase 2 respectively. Grey triangles connected by grey dotted lines mark two examples of "semi-equilibrium," where the chemical potential difference between the components is the same in two phases, but one phase or the other is more stable.

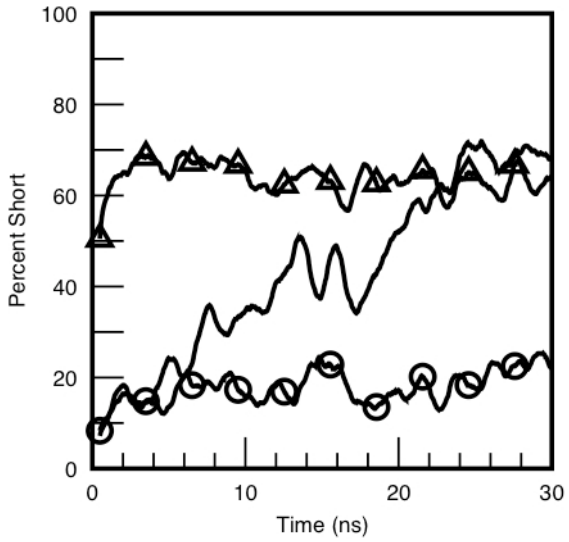

Figure 9. *Percent DMPC in MC-MD simulations of mixed DMPC/DSPC bilayers vs. Time.* Percent DMPC in systems initiated with a 100% DSPC gel structure with activity ratios of 1.0×10^4 and 1.2×10^4 are shown as curves outlined with circles and without, respectively. Percent DMPC in a system initiated with a 100% DSPC LC structure with an activity ratio of 1.0×10^4 is shown outlined with triangles. The curves in both panels represent running averages over 1 ns.

According to experiment, at 313 K the LC and gel phase coexistence boundaries are at ~64% and ~10% DMPC.(2, 45) The simulated "semi-equilibrium" pairs that come closest to the true experimental boundaries are found at activity ratios of 1.0×10^4 (64% DMPC in LC, 21% DMPC in gel) and 0.8×10^4 (57% DMPC in LC, 12% DMPC in gel). In either case, the simulation predicts a coexistence region that is narrower by about 10 mole% than observed experimentally. It is not surprising that the current model does not match experimental phase behavior exactly, given how sensitive phase boundaries are to details of molecular structure and interactions: even as small an experimental perturbation as perdeuteration of the tail chains shifts T_m by five degrees K.(45)

2.4 Conclusions

The present semi-grand canonical ensemble simulations constitute a first effort to use atomistic simulation to study the details of mixed-lipid bilayers in the gel phase, unhindered by the slow dynamics of lateral diffusion. Within a gel phase dominated by the longer-tail DSPC lipid, the DMPC molecules in these simulations tend to associate with one another and to shift towards the bilayer midplane, but not enough on average to bring their tails' terminal methyl groups as far down as DSPC. These behaviors are in stark contrast with the behaviors of the shorter-tail component in fluid-phase mixtures, where lateral distributions appear to be random and where the headgroups of long and short lipids occupy an unbroken layer.

The ability to determine composition from activity ratio independently from gel and LC phases yields partial information about the coexistence between gel and LC phases of different compositions. While the precise limits of the coexistence curve cannot be obtained due to the slow rate of transition between the phases, the present results suggest that the coexistence region for the simulation model is narrower than the true experimental value. Given that the main transition temperature for the current potential is in error, as noted above, by an estimated 10 K, this discrepancy is not surprising.

In further work, the temperature dependence of the mixing behavior, and particularly of the apparent coexistence boundaries, will be investigated; among other questions, the miscibility within the gel phase, at temperatures below both components' transition temperatures, is of interest. Furthermore, the structure of gel-phase mixtures containing

unsaturated lipid tails is a related topic that may be addressed by the MC-MD method. Finally, the influence of cholesterol on this phase transition and the structures of ternary mixtures in the LC, gel, and liquid ordered phases are of significant interest.

3 Determination of Phase Transition Temperatures of Atomistic Model Lipid Bilayers from Temperature-Dependent Stripe Domain Growth Kinetics

3.1 Introduction

Much has been learned about the phase behavior of lipids, the primary component of biological membranes, in the past few decades. One contributor to interest in this field is the hypothesis that ordered lipid domains called rafts are central to many biochemical processes.(46-50) Computer simulation has been an important tool in the investigation of lipid bilayers, providing details that are generally inaccessible to experiments. Most force-fields used in the study of lipid bilayers were originally developed for the fluid liquid crystalline (LC) phase, but have proven to be transferable to the more ordered gel phase(17, 51) as well as intermediate phases(20) reproducing structural features with generally good success. It is more difficult to validate the ability of a force-field to reproduce the thermodynamics of the ordering process, the main transition temperature T_m being the most relevant quantity, because transitions between the two phases are slow on the simulation timescale, particularly near T_m. Insight about how well force-fields agree with experimental phase behavior of single-component lipid systems is desirable for the interpretation of simulation data pertaining to more complex ordered phases such as the cholesterol-containing “liquid ordered” structure.(52-54)

Two recent attempts at calculating T_m have been published, both using the same popular united-atom force-field of Berger et al.(32) Leekumjorn and Sum simulated annealing a fully hydrated DPPC bilayer from 250 to 350 K and back to 250 K.(21) Plotting area per lipid as a function of temperature revealed a loop of hysteresis with a crossover between two linear regimes, most evidently in the heating trajectory. The intersection of the linear portions was identified as the transition temperature, found to be 10°C below the experimental main phase transition temperature ($T_{m,exp}$), 315.2 K.(55) Qin, *et al*, used similar annealing runs, plus long trajectories over a range of fixed temperature points, to estimate a T_m of 299 K for DSPC, 30° below experiment.(55, 56) The very significant degree of hysteresis in the annealing runs makes the identification of a transition temperature quite difficult, and potentially dependent on the rate of heating and cooling. Part of the reason for this hysteresis is the interfacial free energy barrier that must be surmounted in the nucleation of a new phase. A recent coarse-grained study suggested the gel-LC transition occurs in 4 distinct steps: (i) phase nucleation, where 20-80 lipids congeal and form a gel domain within the bulk LC, (ii) fast growth, where the number of lipids added to the gel domain increases rapidly, (iii) slow growth, in which gel domains start to percolate, and (iv), optimization, where trapped LC domains persist on the microsecond time scale, and defects are eventually resolved.(15, 57) The size and time limitations of atomistic studies suggest that---of all the above steps---step (ii), fast growth, is the most practical to study.

This report describes an approach to evaluating T_m within a molecular simulation of a lipid bilayer based on a strategy of isolating the "fast growth" stage. This simple method consists of preparing a system consisting of gel and fluid phases coexisting in adjacent stripes, and observing the rate at which one phase or the other grows as a function of temperature. Our aim in using pre-existing stripes is to permit molecules to undergo phase changes without either creating a new interface, which is expected to involve a high free energy barrier, or changing the length of existing interfaces, which would introduce a bias due to interfacial line tension. Results from this method for both DPPC and DSPC bilayers suggest transition temperatures that are ~6-7 K lower than experiment. Possible sources of systematic error and reasons for the discrepancy with estimates taken from annealing trajectories will be discussed. Finally, we will comment on the structure of the interface and the rate of transition near the transition temperature.

3.2 Methods

3.2.1 *Simulations*

Two-phase System Construction: The two-phase (stripe) systems were based on gel structures constructed as follows: two lipids were patterned after the two unique lipids in the crystal structure of DMPC,(25) with two methylene carbons added per tail using Spartan molecular modeling software (Wave Function, Inc.). The remainder of the system preparation was done with GROMACS 3.2.(30, 58, 59) The molecules were oriented in the simulation box with the *z*-axis corresponding to the bilayer normal and the primary axis of the acyl tails in the *yz*-plane. The two lipids were rotated 180° about the *y*-axis and translated in the *x*-axis to make the lipid tails' primary axes collinear. The

four resulting lipids were copied and translated in the *x*- and *y*-axes to achieve hexagonal packing of the lipid tails with an area per lipid of 44.7 Å^2. For the DPPC gel, the 8-lipid configuration was then quadrupled in *x*, hydrated with 25 SPC waters per lipid, minimized over 100 steps via the method of steepest descents, and incubated with molecular dynamics (MD) for 10 ns at 273 K. The resulting configuration was doubled once again in *x* and *y*, and this 128-lipid system was run for another 10 ns at 293 K. The area per lipid evolved to 52 Å^2, consistent with values previously reported.(51, 56, 60) The DSPC gel was constructed in almost exactly the same way. The 8-lipid

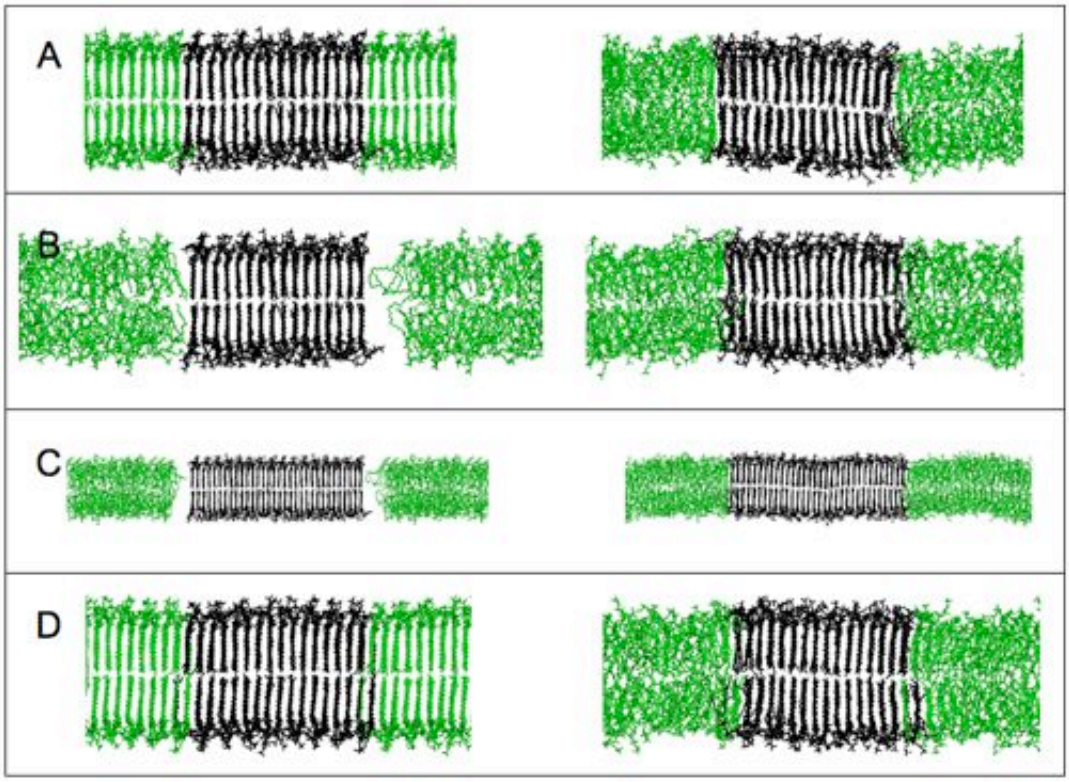

Figure 1. *Constructs Before and After Equilibration.* Systems were prepared from all-gel (panels A and D), or pre-equilibrated gel and LC (panels B and C). Panel A shows a 256-lipid DPPC system, B a 256-lipid DPPC system, C a 512-lipid DPPC system, and D a 256-lipid DSPC system. All panels show the system before equilibration (left) and after (right).

configuration was doubled twice in *y* and once in *x* to make a 64-lipid configuration, which was minimized and run at 313 K for 10 ns, then doubled and run for another 20 ns, again at 313 K. The area per lipid of the final structure was 52 $Å^2$.

Two methods were used to prepare two-phase systems. In the first, referred to below as the "*m*" method, the pre-equilibrated gel was incubated with half the lipids (divided along one axis) set at 293 K, and the other half (and solvent) set at 353 K for 10 ns (see fig. 1 A). In the second, referred to below as the *"p*" method, two 128-lipid pre-equilibrated bilayers, gel and LC, were combined side-by-side within a simulation box, with adequate space to avoid overlaps, and run for 10 ns (see fig. 1 B). The temperatures of the gel, the LC and solvent were set to 293, 353 and 353 K, respectively, as before. Areas per lipid and fraction of tail dihedrals in the *trans* conformation reached plateau values within 10 ns (data not shown). The stripe DSPC system was constructed as described above except that the gel and LC/solvent were run at 303 K and 363 K, respectively (see fig. 1 D).

All MD simulations were run with GROMACS 3.3 and 3.4(30, 58, 59) and the following parameters. The Berendsen barostat(34) was used for anisotropic pressure coupling, with box dimensions and angles free to adapt independently to the stresses in the system. The reference pressures were 1 bar with all compressibilities set to 4.5×10^{-5} bar^{-1} and a time constant of 2 ps. Langevin dynamics were used for the thermostat,(35) with a time constant of 0.2 ps. Interaction cutoffs (neighbor lists, van der Waals radii, and coulombic cutoffs) were all set to 1.0 nm. Electrostatics were calculated with Particle Mesh Ewald

sums.(61) A time step of 2 fs was used. Both the DPPC and DSPC systems were run at a range of temperatures listed in Table 1.

DSPC cooling: A previously equilibrated system containing 128 DSPC lipids and 3200 water molecules in the fluid phase(51) was cooled from 333 K, above the experimental main phase transition temperature of 328 K, down below 300 K at various rates; 1 K/ns, 0.5 K/ns, 0.2 K/ns and 0.1 K/ns.

lipid	temperature (K)	number of lipids-construction method	simulation length (ns)
DPPC	293	256-*m*	100
DPPC	298	256-*m*	100
DPPC	300.5	256-*m*	100
DPPC	303	256-*m*; 256-*p*; 512-*p*	160; 100; 20
DPPC	308	256-*m*; 256-*p*; 512-*p*	100; 100; 20
DPPC	310.5	256-*m*	100
DPPC	313	256-*m*	100
DSPC	313	256-*m*	100
DSPC	318	256-*m*	100
DSPC	320.5	256-*m*	100
DSPC	323	256-*m*	100
DSPC	325.5	256-*m*	100
DSPC	328	256-*m*	100

Table 1. *Description of Systems Simulated.* Construction methods *m* and *p* are described in Methods.

3.2.2 *Analysis*

To calculate phase amounts, a lipid was classified as belonging to the gel phase if it---and at least 4 of its nearest-neighbors---had a maximum of 2 gauche tail dihedrals. The nearest-neighbor criterion was used to eliminate error due to transient ordering of a lipid, which can happen in the LC phase. The lipid gel fraction was plotted against simulation

time. A linear regression of these curves gives a line whose slope is the rate of change; since the simulation boxes have two-phase interfaces, the rate of interface translation is the rate of change of phase composition multiplied the width of the simulation box (in nm) divided by two. These curves were divided into uncorrelated samples by the method described in Allen and Tildesley,(62) section 6.4, yielding segment lengths between 1 and 9 ns, and error bars represent the standard error of the slopes calculated over uncorrelated segments of the trajectory.

3.3 Results

3.3.1 *Lipid Bilayer Annealing*

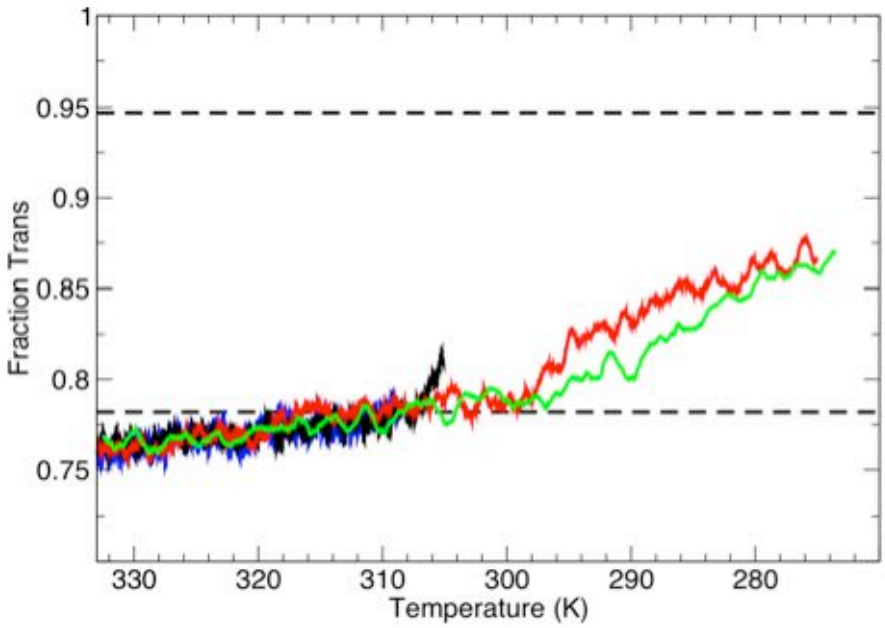

Figure 2. *DSPC Tail Order vs. Temperature.* A pre-equilibrated DSPC LC cooled at different rates; shown is the time evolution of fraction of tail dihedrals in the trans conformation for simulations run at 1 K/ns (green), 0.5 K/ns (red), 0.2 K/ns (black), and 0.1 K/ns (blue), all 1 ns running averages. For comparison, 50 ns averages of gel (at 0.95) and LC (at 0.77), both run at 313 K, are shown by black, dashed lines.

In principle, a gradually cooled lipid bilayer should undergo a phase transition at a characteristic temperature T_m. At least two previous simulation studies have aimed to determine T_m through this approach.(21, 56) In both cases, a pre-equilibrated LC system was cooled at 2.5 K/ns. To investigate the reproducibility of this method, DSPC was cooled from 333 K, 5 K above the experimental T_m ($T_{m,exp}$) at even slower rates---1, 0.5, 0.2, and 0.1 K/ns. The fraction of acyl tail *trans* dihedrals initially increased slowly with decreasing temperature (fig. 2). As in the previous studies, a change in slope was observed upon reaching a sufficiently low temperature. However, two observations indicated that the results were influenced strongly by the kinetics of forming a new phase: the temperature where the change in slope was observed was sensitive to the rate of cooling, and further cooling down to 273 K (for 1.0 K/ns and 0.5 K/ns trajectories) failed to produce a uniformly ordered gel phase.

To avoid the uncertainties associated with the annealing method, an independent method of obtaining T_m within a simulation model was applied. As described in the Methods section, the "stripe-growth" method involves preparing a system composed of alternating stripes of gel and LC domains and observing the dynamics of domain growth in independent simulations over a range of temperatures.

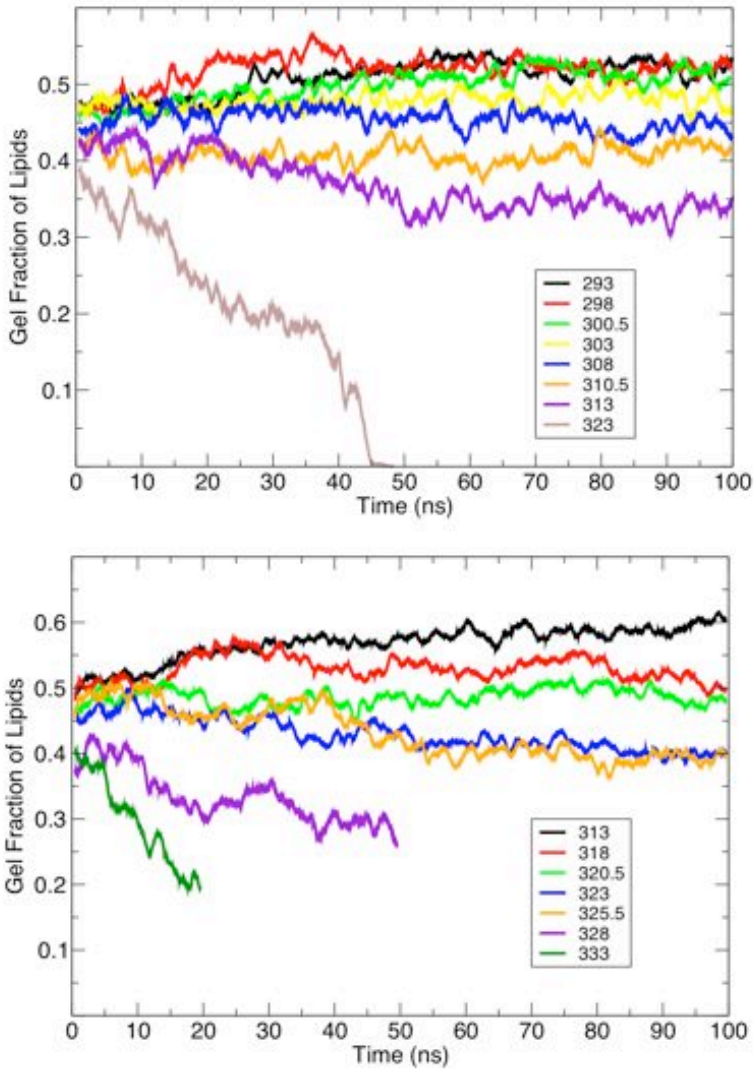

Figure 3. *Gel Fraction of PC Lipids over a Range of Temperatures.* The fraction of total lipids (DPPC, top panel, and DSPC, bottom panel) qualifying as gel is plotted as a function of time. 1 ns running averages are shown.

3.3.2 *Qualitative analysis of gel-LC transition*

Two-phase simulations of both DPPC and DSPC run at several temperatures (Table 1) show that the speed and direction of the phase transition changes with temperature, as indicated by plots of gel fraction versus simulation time (fig. 3) and snapshots of simulation endpoints (fig. 4). The DSPC simulation at 313 K, for example, exhibits a visible widening of the gel stripe, while at the highest temperatures studied (328 and 333

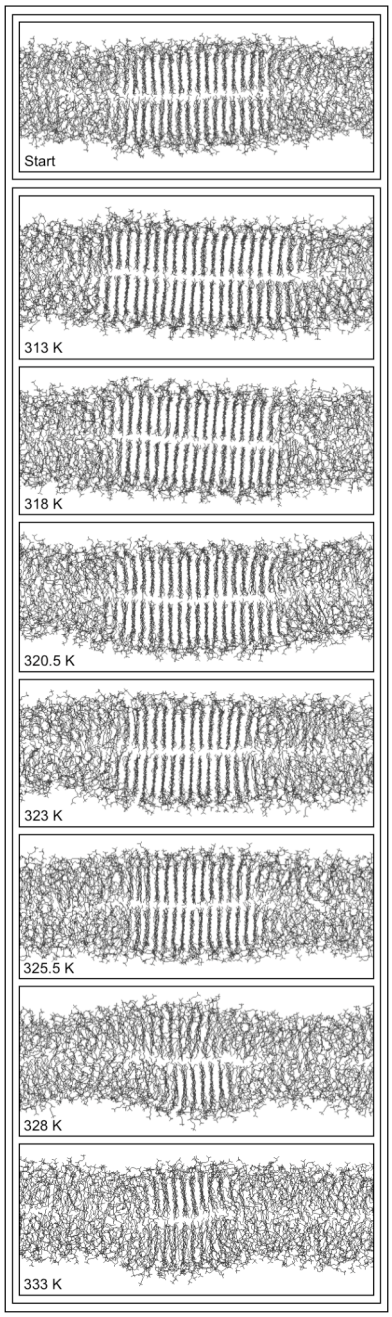

K) the gel is plainly melting at the interface. At intermediate temperatures the trend is not immediately obvious. By gross qualitative measures, the two-phase method appears to indicate a T_m between 313 and 328 K for the DSPC model, a range beginning 15 degrees below the experimental $T_{m,exp}$ and extending up to $T_{m,exp}$.

Figure 4. *Snapshots of DSPC Two-Phase Systems.* Snapshots of all temperatures used for simulations are shown as labeled. The top panel is the system at t = 0 ns. The bottom panel shows the systems at 100 ns: (in descending order) 313 K, 318 K, 320.5 K, 323 K, 325.5 K, 328 K, and 333 K.

Visual inspection of stripe trajectories yields further insight into structural details of the phase transition. At all temperatures, changes in lipid order were localized at the gel-fluid interface. Even for DPPC at 313 K, where the gel phase melted completely, melting occurred from the boundary inward. This observation is consistent with the notion that phase nucleation is a rate-limiting step. Snapshots of a DSPC interface at 313 K (fig. 5) reveal that lipids that have transitioned from a LC to a gel at the interface exhibit decreased lateral orientational order, relative to those in the pre-prepared gel stripe. The snapshots are sighted down the tails' primary axis to highlight their arrangement in a hexagonal array. As described in Methods, within the constructed gel phase, lipids are arranged in well-defined rows with their glycerol

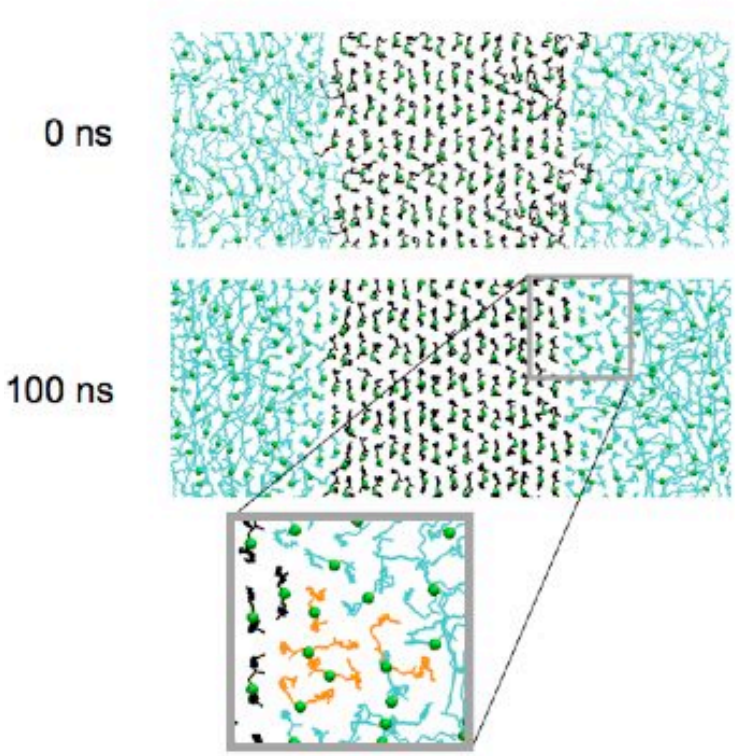

Figure 5. *Gel-LC Interface Below T_m.* The glycerol backbone and acyl tails of a DSPC system simulated at 313 K are shown at t = 0 ns (top) and t = 100 ns (bottom). For clarity, only one leaflet is shown, the headgroups are hidden, and the leaflet is rotated so the view is down the axis of the gel tails. Molecules are colored for their starting phase---gels are black and LCs are cyan. To underscore molecular orientation, carbon #13 (of the glycerol backbone) is depicted by a green sphere. The magnified field shows 5 gel lipids that started as LCs re-colored in orange to highlight their disordered tail packing.

backbones parallel to the stripe dimension. In contrast, lipids that congeal at the interface do not conform to this arrangement. Although the tails still form a hexagonal array tilted parallel to the stripe dimension, the two tails of a given lipid may not lie in the same row, and may not even occupy nearest neighbor sites within the hexagonal lattice. Fig. 5 displays this arrangement in the magnified field from the 100 ns time frame at bottom. For example, of the five lipids colored in orange, the top left lipid appears to have congealed following the same pattern of the original gel. But the one at bottom left is turned 60° in the plane perpendicular to the tails. Its two tails occupy separate rows.

Two other lipids, the second from top on left and the rightmost, deviate even more from the original packing pattern; both of them have non-nearest neighbor tails. Similar disordering at the interface is also seen during melting.

3.3.3 *Quantitative measurement of domain growth*

The average rate of expansion or retraction of the gel phase edges for DPPC and DSPC at each temperature, as described in Methods, was estimated by linear regression from the data in fig. 3 and is plotted in fig. 6. We find that an equation with three adjustable parameters

$$\text{rate} = A'' \cdot (T_m - T) \cdot \exp(-E_a / RT) \qquad \text{(Eq. 1)}$$

provides reasonable fits to the data. This equation makes phenomenological sense if we consider the conversion between phases to be an activated process with activation energy E_a and a driving force proportional to the difference in free energies between the phases, which is proportional to T_m-T close to the transition temperature. In contrast with both experimental and simulated domain growth kinetics that include a nucleation step followed by growth of compact domains,(15, 57) line tension does not appear as a parameter in the current model because stripe broadening does not change the length of the interface. A least-squares fit of the data to Eq. 1 (shown in fig. 6) yields estimates of A'', E_a, and T_m (see Table 2). Apparent activation energies are near 70 kJ/mol in both systems. Interconversion between gel and LC conformations involves a large conformational change to the lipid tails. With the torsional barrier of about 10 kJ/mol

between *gauche* and *anti* structures for each tail dihedral, this activation energy could be interpreted as an indication that the transition requires cooperative rearrangements involving seven torsional angles within the tails.

	A'' (nm·ns^{-1}·K^{-1})	T_m (K)	E_a (kJ/mol)
DPPC	1.99×10^{9}	308.5	68.4
DSPC	2.60×10^{10}	323.4	75.6

Table 2. *Best Fit Parameters.* The rates of phase transition for DPPC and DSPC systems were fit to Eq. 1, giving values shown here.

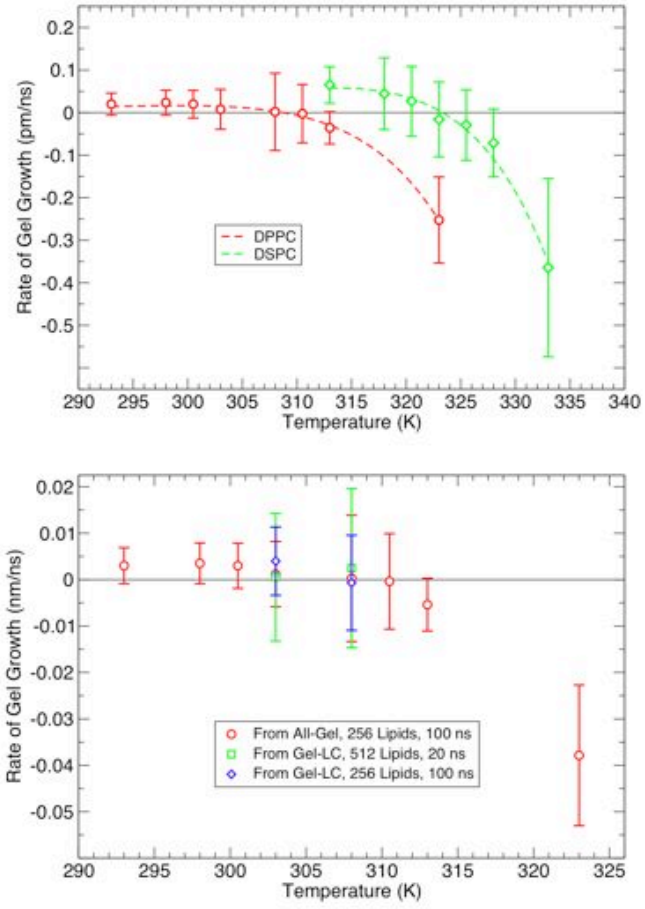

Figure 6. *Main Phase Transition Rates vs. Temperature.* The rates of transition of DPPC (red) and DSPC are shown in red and green, respectively (top panel). Open circles are the rates calculated by the gel qualifier method, and hashed line is the best fit. The rates of main simulations of DPPC are compared with the DPPC controls (bottom panel).

The transition temperatures calculated from fits to eq. 1, 308 K for DPPC and 323 K for DSPC, are closer to their experimental transition temperatures than the previous studies have suggested. Leekumjorn and Sum estimated the T_m of DPPC using this force-field to be 10 K less than the experimental T_m,(21) and Qin, et al,(56) estimated the T_m of DSPC---with the same force-field---to be 29 K less than the experimental T_m. The present study suggests that the simulation model may underestimate the T_m by as little as 7 K for DPPC and 6 K for DSPC.

While the primary goal of this study was to estimate T_m, the actual values of the rates of domain growth are also of interest. An experimental study(57) indirectly established that, within 5 K of T_m in DPPC, the interface travels at a rate proportional to $(T - T_m)$, with a constant equaling 0.002 nm·ns^{-1} K^{-1}; the corresponding constant from the present fit would be given by $A'' \exp(-E_a/RT_m) = 0.005$ nm·ns^{-1} K^{-1}, in fair qualitative agreement. A coarse-grained model study reported linear dependence of domain growth with a slightly higher coefficient, 0.007 nm ns^{-1} K^{-1}.(15)

3.4 Discussion

A plausible explanation for why the stripe-growth method yields a higher T_m than annealing methods lies in the stability of the gel phase. During relatively rapid heating/cooling loops, optimal packing of the gel lipids is probably not achieved, as evident in the regions of disorder characteristic of the starting fluid phase (not shown) that persist even at temperatures well below the apparent T_m. Thus, the stabilities of

the gels will tend to be underestimated by heating/cooling loops. In one study, an ordered phase formed with different orientations of lipid tails in the two layers during a deep quench to 250 K.(56) While this structure may represent the thermodynamic free energy minimum well below T_m, if it is metastable close to T_m it too will melt at a lower temperature than would a more stable ordered structure. Assuming that the high-temperature phase equilibrates more rapidly than the low-temperature phase, estimates to T_m in poorly equilibrated systems will generally be too low.

The stripe-growth method is itself subject to several potential sources of error in calculating T_m. It replaces the uncertainties of generating a gel phase through quenching with uncertainties associated with initial construction of a model gel phase domain, some details of whose equilibrium structure are unknown, and on an initial preparation of a gel-LC interface, about which even less is known. In an attempt to control for the effects of how the initial interface is prepared, stripe systems were prepared in two different ways, first by melting half of the lipids in a pre-equilibrated gel (fig. 1 A), and then by flanking pre-equilibrated gel with pre-equilibrated LCs (fig. 1 B). The rates of phase-change were the same within statistical error (fig. 6, bottom panel). Finite-size effects are also a concern in studies with interfaces. Specifically, how far do the effects of the interface extend into the bulk? And equivalently, are there lipids far enough from the interface that they exhibit true bulk properties? This is addressed by comparing the phase-change rates of the constructs with different phase widths (fig. 6, bottom panel). No significant difference was identified between the small and large systems.

An open question about the current data is why the initial rates of gel phase growth or disappearance slow down over the course of the trajectory, resulting in a leveling off of most of the curves in fig. 3. This diminishment suggests that over time, either the driving force for further transitions goes down or the barrier goes up. The driving force for the conversion of one phase to another could change over the course of the trajectory due to finite-size effects; the rate may depend on the width of one phase or another. As stated above, the simulations on a system that is twice as wide do not seem to corroborate this; neither does the observation of diminishing rates for both gel growth and gel disappearance. Rather, we hypothesize that the barrier for changing the position of the interfacial front increases over the course of the trajectory as the interface becomes increasingly stable through some slow relaxation process. In fact, the observed reordering of the interface (fig. 5), both during congealing and melting, is indicative of such a relaxation process. The gradual change in interfacial structure would reduce the rate of phase growth in both directions, affecting our estimates for the absolute rate of interfacial growth. The implications of such a change for the estimates of T_m are not clear. In principle, the direction of spontaneous phase transition is independent of the details of the interface; in practice, it is difficult to rule out the possibility that the restructuring of the interface may influence an apparent phase growth. The uncertainty about the structure of the interface, and the computational expense of simulating long time intervals make this last concern the most difficult to address.

3.5 Conclusions

Determination of the main phase transition temperature of lipid bilayers simulated with atomistic force-fields is a an important step in force-field validation.(21, 56) In the present study, the rates of phase growth in coexisting gel and LC phases pre-formed into stripes has been investigated as a new way of obtaining the main phase transition temperature T_m. Our results indicate T_m values that are higher, and in closer agreement with experiment, than are obtained through annealing studies. The use of a linear phase interface allows the measurement of rates of domain growth, yielding an estimated activation barrier of 70 kJ/mol for the transition, with absolute rates of the same order of magnitude as determined by experiment.(57) Inconsistency in rates over the course of 100 ns simulation trajectories may be related to structural evolution of the gel/LC interface from an initial state with aligned glycerol backbones to a rougher structure with orientational defects. Whether this disorder is localized at the interface and acts as a barrier to further growth, or whether such disorder is in fact more characteristic of the bulk gel state than the ordered structure originally prepared, remains a question for future study.

4 Order in the Glycerol Backbone of the Gel Phase of Phosphatidylcholine

4.1 Introduction

The phase behavior of phosphatidylcholine (PC) lipid bilayers has been studied for decades.(25, 40, 63-67) The following general picture has long been clear. Upon hydration and heating, the diacylphosphatidylcholine crystalline (L_c) phase undergoes a phase transition to the gel phase ($L_{\beta'}$): the headgroups become disordered while the tails retain their hexagonal packing order, the area per lipid increases from 40 to ~50 Å^2, and the tail tilt increases from 12° to ~30°. The "main phase transition", so called because it is the only phase transition that is observed without regard to system history, occurs between the $L_{\beta'}$ and the liquid crystal (LC, or L_α) phase (fig. 1). The LC has a larger area per lipid (~65 Å^2) and, perhaps most significantly, the tails undergo large conformational disordering and lose their collective tilt. For an excellent review of lecithin phase character, see Koynova and Caffrey.(67)

While the LC phase (and cholesterol containing liquid-ordered phases,(49, 54)) are believed to be of greatest relevance to cell membranes, molecular dynamics simulations of PC lipids in the gel phase provide useful tests of force-field accuracy due to the availability of specific experimental structural parameters for comparison, such as those listed in Table 1. Three angles are needed to characterize the orientation of a tail within the gel structure. The tilt angle θ is defined as the angle between the overall tail vector

and the bilayer normal (illustrated in fig. 2, top left); experiments show that this angle does not depend strongly on the tail length in the range from DMPC (di-C_{14} tails) to DSPC (di-C_{18} tails). The tilt direction can be defined in terms of the angle ϕ (fig. 2, top right) between the projection of the tail vector onto the plane of the bilayer and the vector between nearest neighbors in the hexagonal lattice formed by the tails. X-ray scattering experiments indicate that the tilt direction is toward nearest neighbors, $\phi = 0$.(68) Finally, the tails are not smooth cylinders; the rotation of the hydrocarbon tails can be described by the angle γ between the plane containing the carbon-carbon bonds in the tail and the plane described by the tail-tilt direction and the bilayer normal (fig. 2, bottom left). Experiments suggest that tails adopt a broad distribution of γ angles, but peaked at $\gamma = 90°$.(69)

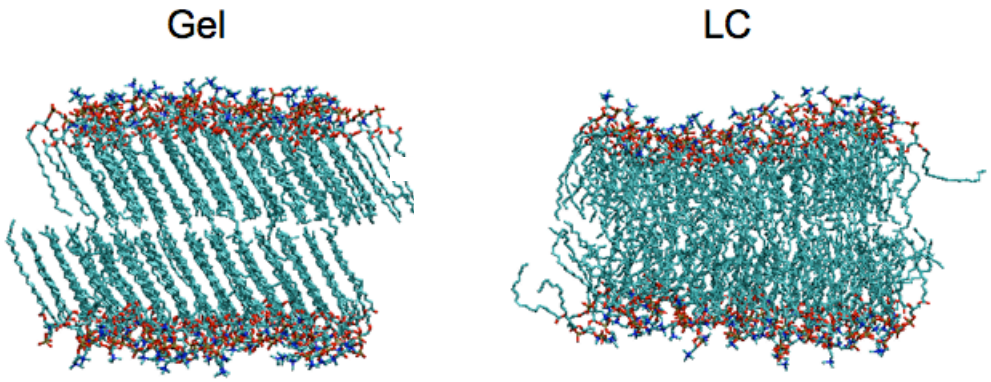

Figure 1. *Gel and LC Snapshots*.

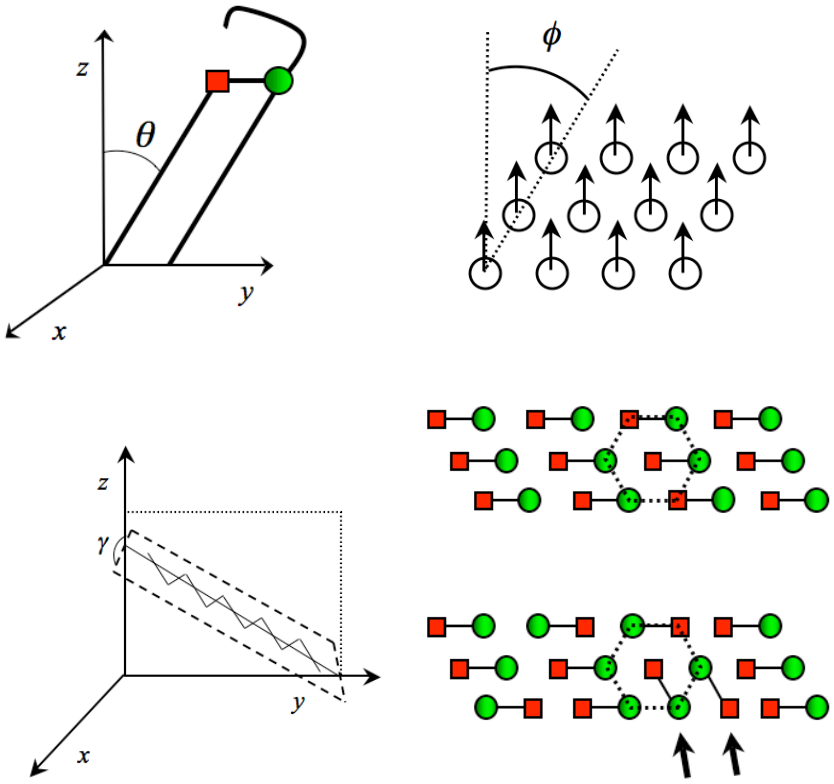

Figure 2. *Orientational Parameters*. An idealized PC lipid is shown at top, left. The red square and green sphere represent carbon 13 and carbon 34 of the glycerol backbone, the junction points for tails 1 and 2, respectively. The *z*-axis here is the bilayer normal, and the angle between it and the primary axis of the tails is the tail-tilt direction θ. Tail-tilt direction is illustrated in the diagram at top, right. The circles represent tail centers of mass and the arrows show direction of tilt. Tail-tilt "direction" is defined by the angle ϕ between tail-tilt direction and the nearest neighbor projected onto the *xy*-plane. A cartoon of an acyl tail is shown at bottom, left. Its primary axis is in the *yz* plane for clarity. γ is the angle between two planes: the first defined by the bilayer normal (*z*-axis, here) and the tails primary axis (shown with dotted lines), and the second in which the C-C bonds lie (shown with hashed lines). At bottom, right are two arrays of four lipids, one (top) is ordered, the other (bottom) is disordered.

While the ordered tail structure of gels is amenable to experimental characterization by X-ray or neutron scattering, the nature of the disorder in the remainder of the molecule (the glycerol backbone and the phosphocholine headgroup) is more difficult to describe. The crystalline phase features neat rows of molecules, with all glycerol backbones aligned and oriented in the same direction within the hexagonal lattice and headgroups alternating between two well-defined conformations. Experimental evidence from x-ray

and neutron scattering studies suggest orientational disorder of the glycerol backbones in the $L_{\beta'}$ phase of DPPC,(70, 71), as shown in fig. 2, bottom right, with a "sub-gel" $L_{c'}$ phase having a regular order to the glycerol backbone arrangement that may be different from the L_c phase.(71) Lateral disorder was also observed in the glycerol backbone arrangement of lipids undergoing a transition to the gel phase in recent atomistic simulations,(72) even when these were being added to an existing well-ordered domain.

Making an atomistic model of the gel phase is not trivial. Simulated annealing from an LC phase is a long and uncertain process, which tends to produce bilayers with gel domains interspersed with significantly disordered regions (21), or gels without a uniform tilt angle (56), although one reported 300 ns simulation at a very low temperature resulted in a uniform gel structure.(20) Most researchers, starting with the first attempt at a gel-phase simulation of POPC by Heller et al. in 1993,(73) have prepared the gel-phase structure by construction, often(17-19, 74) using the crystal structure(25) as a starting point. Reorientation of the glycerol backbone within the gel phase is too slow to observe during a molecular dynamics simulation,(71) so---even more than LC simulations---gel simulations are strongly biased by starting configurations. We find that simulations of model DSPC (distearoyl phosphatidylcholine) gels with different initial degrees of glycerol orientational order lead to equilibrated configurations with measurably different structural and thermodynamic properties. Here we present the differences in these properties, and show that they are strongly coupled to the glycerol backbone configuration. An important implication is: using the crystal structure of a phospholipid as the starting configuration for gel phase simulations could lead to misleading results.

4.2 Methods

4.2.1 *Configuration construction*

DSPC Glycerol Backbone Disordered (BD)

The crystal structure of DMPC(25) was used to construct two unique lipids extending the tails by 4 carbons each, in the same manner as Tu et al.(17) The two lipids were rotated 180° in the plane of the tail-tilt (*zy*, where *z* is the normal of the bilayer) and translated such that the tails of the "top" two lipids were collinear with the tails of the "bottom" two. This 4-lipid structure was then copied and translated in the two axes that describe the bilayer plane(74) (*x* and *y*), such that the tails pack hexagonally with an area per lipid of 48.2 $Å^2$. The resulting 8-lipid structure was doubled twice in both *x* and *y*. This 64-lipid bilayer was solvated with 3200 SPC waters(31) and equilibrated at 313 K for 10 ns. The equilibrated 64-lipid system was doubled in *x* and *y*, and a square patch of 128 lipids was cut out and equilibrated for 50 ns (see fig. 3, left).

One subtle element of disorder beyond the alignment and ordering shown in fig. 2 is as follows: all previously reported simulations have assumed the tails of a given lipid occupy adjoining positions in the hexagonal lattice. That is not the case with BD; there are some tails that occupy next-nearest-neighbor sites in the lattice. Such defects were also observed in the lipids that were deposited at the gel-LC interface in the phase-propagation paper recently reported by our group (submitted).

DSPC Glycerol Backbone Ordered (BO)

The first 8 lipids were constructed exactly as with BD, except they were packed with an area per lipid of 44.7 $Å^2$, to give the tails regular-hexagonal packing. This structure was doubled twice in *x* and once in *y*, solvated with 3000 SPC waters, minimized with steepest descents, and equilibrated for 10 ns at 313 K. It was then doubled in both *x* and *y*. yielding a 128 lipid structure, which was then equilibrated for 50 ns (see fig. 3, right).

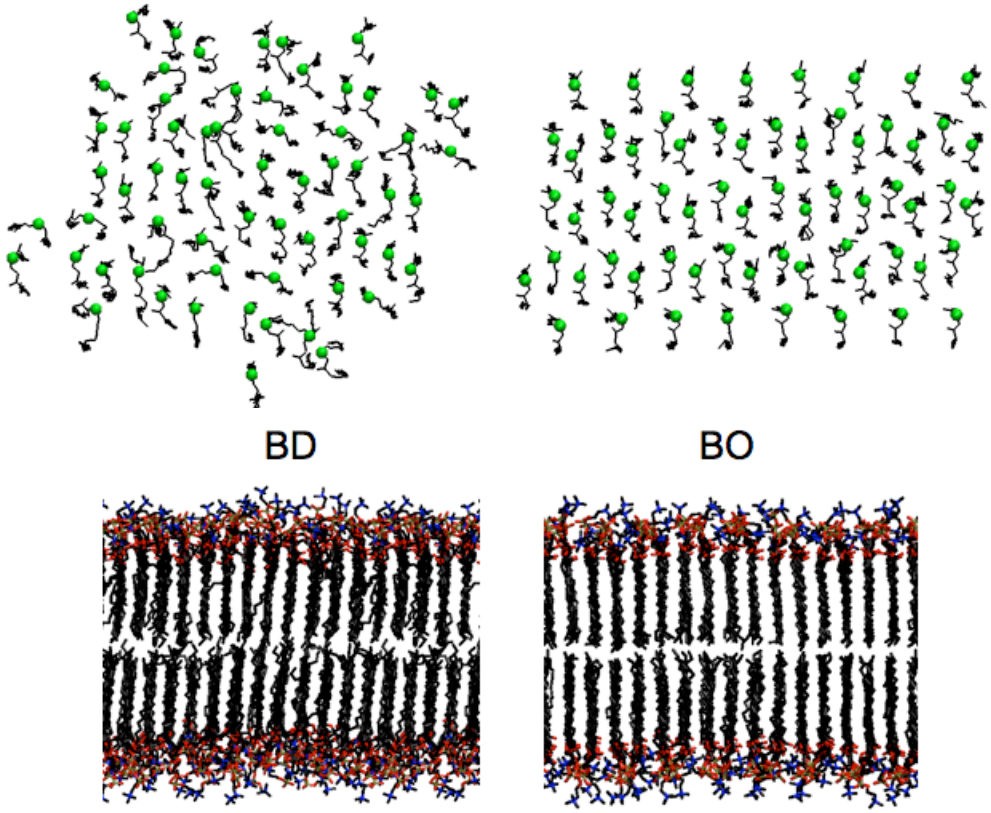

Figure 3. *Snapshots of the Two Gels, Glycerol Backbone Disordered (BD) and Glycerol Backbone Ordered (BO).* A view down the tail primary axes shows lateral arrangement of the two structures (top). Only one leaflet is shown, and headgroups have been removed to clarify the glycerol backbone orientations. Carbon 13, the junction point of the glycerol with tail 1, is shown as a green sphere to indicate orientation, and tails are shown in black. The bottom pictures are of the gels looking in the direction of the tail tilt. I.e., the tail is tilted into (or out of) the page.

4.2.2 *Simulations*

Molecular dynamics (MD) simulation were performed as have been reported previously. The first gel, hereafter referred to as "BD" (backbone disordered), was reported by Coppock and Kindt.(51) Both systems used a Berendsen barostat,(34) BD with semi-isotropic pressure coupling with a reference pressure of 1 bar, compressibilities of 4.5×10^{-5} bar^{-1} and a time constant of 2 ps. The second gel, "BO", for **b**ackbone **o**rdered,(72) was run with anisotropic pressure coupling with the same reference pressure, compressibilities, and time constant. Otherwise, all simulations were run with GROMACS 3(30, 58, 59) using the same parameters: a Langevin thermostat(35) with a temperature of 313 K and a coupling constant of 0.2 ps, PME electrostatics(61) with cutoffs (van der Waals, neighbor lists, and coulombic) of 1.0 nm. The united-atom force-field described by Berger et al was used,(32) with a time step of 2 fs. Both systems were equilibrated for 50 ns, the last 10 ns of which were used for analyses.

Mixing simulations were also performed on both gels by a method described previously.(23, 36, 51) Briefly, MD steps were performed alternately with Monte-Carlo (MC) moves. In each step, a lipid is chosen at random. If it is DMPC, a successful move adds 4 methylene carbons to each acyl tail. If it is a DSPC, a successful move removes the last 4 carbons of each tail. Each carbon is added in the following manner: *k* test positions, chosen from a distribution defined according to their bonding and torsional potentials, and are Boltzmann weighted by their non-bonded potentials. The acceptance probabilities are weighted by activity ratios $\alpha = a_{DMPC}/a_{DSPC}$ where $a_i = \exp(\mu_i)$.

Activity ratios reported here are 1×10^4 and 5×10^4, and $k = 4$ test positions were generated for each carbon added to short-tailed lipids. Acceptance ratios were on the order 0.001.

4.3 Results and Discussion

lipid/temp (K)	APL (Å^2)	Thickness (Å)	tilt (°)	tilt direction (°)	method/ref.
DMPC/283	47.2±0.5	40.1±0.1	32.3±0.6	0	x-ray(75)
DPPC/292±1	47.2±0.5		32.0±0.5		x-ray(39)
DPPC/292±2		42	30		x-ray(66)
DPPC/293	45.9±2.0	45.0±1.0	30.0±3.0		x-ray(76)
DPPC/298			32.6	0	x-ray(68)
DSPC/292±1	47.3±0.6		33.5±0.6		x-ray(39)

Table 1. *Structural Parameters of PC Gels Measured by Experiment.* Thicknesses are the distance between the maxima corresponding to each leaflet in the electron density profiles, or headgroup to headgroup.

system/temp (K)	APL (Å^2)	Thickness (Å)	tilt (°)	tilt direction (°)	Percent of gauche 6-dihedrals	rotational order *g*	Ref.
DSPC NPT BD (293)	50.1±0.3	47.1	36.1±0.5	0	2.7±1.4	-0.22	This work
DSPC NPT BD (313)	50.9±0.2	46.0	35.3±0.5	0	4.0±1.8	-0.20	This work
DSPC NPT BD (323)	51.8±0.3	47.9	35.1±0.4	0	4.5±1.9		This work
DSPC NPT BO (313)	52.7±0.2	43.3	42.5±0.4	0	0.6±0.7	-0.28	This work
DPPC NPT (292)	45.8	45.6±0.8	33.6	30			(17)
DPPC NPAT (293)	45.7		32.3	0			(18)
DPPC NPγT (293)	45.4		31.9	0			(18)

Table 2. *Structural Parameters of PC Gels from Simulation.* The first four simulations were performed with all-atom force-fields. The last four, from this study, were performed with united atom force-field. The thickness is the difference between average phosphorus position, with respect to the normal, in each layer.

4.3.1 *Effect of backbone order on gel structure*

Equilibrated gel-phase structures of DSPC from the current simulations give higher tilt angles and areas per lipid (and correspondingly, lower thicknesses) than values determined by x-ray diffraction. By each of these measures, agreement with experiment is better for the disordered gel structure (BD) than for the fully ordered structure (BO) (see Tables 1 and 2). Differences associated with the initial glycerol backbone order at fixed temperature are greater than differences associated with temperature over a 20 degree range.

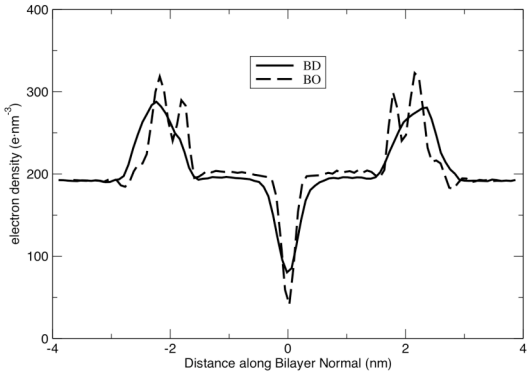

Figure 4. *Electron Densities along Bilayer Normal.* Electron density distribution profiles are shown here as a function of distance form the bilayer mid-plane.

Electron density profiles of the gels (fig. 4) reveal a bimodal distribution of the headgroup electron density in BO, more like the crystal structure than the gel.(25, 76) The electron density profile of BD is similar to X-ray scattering experiments.(76) The acyl tails of BO appear to be packed more densely than of BD, although in both cases tails were packed hexagonally and with tails tilted towards nearest neighbors ($\phi = 0°$), consistent with experimental studies of gels at full hydration(68, 75).

As should be expected, tail packing density scales with tail order. Order parameter S_{CH} is defined by

$$S_{CH} = \tfrac{1}{2}\left\langle 3\cos^2\theta - 1 \right\rangle \qquad \text{Equation 2}$$

where θ is the angle between the bilayer normal the and r_{ik}, the vector defined by carbons i and k in the carbons chain -C_i-C_j-C_k-. Defining the bilayer normal by the vector (0,0,1),

$$\theta(\mathrm{C}_j) = \frac{\cos^{-1}(r_{ik} \bullet (0,0,1))}{|r_{ik}|} \qquad \text{Equation 3}$$

Fig. 5 shows the order of the tails both with an order parameter S_{CH} (left) and with time evolution of the fraction of tail dihedrals (position 6 in each tail) in the *gauche* conformation (right). As the order parameter depends primarily on the tilt angle, tail conformation is a better indicator of total order. Comparison with results of Raman spectra of DPPC gels at 311 K (38) indicating 2.3±1.1% *gauche* dihedrals at position 6, indicates the tail order of BD (4.0±1.7%) is more realistic than that of BO (0.6±0.7%).

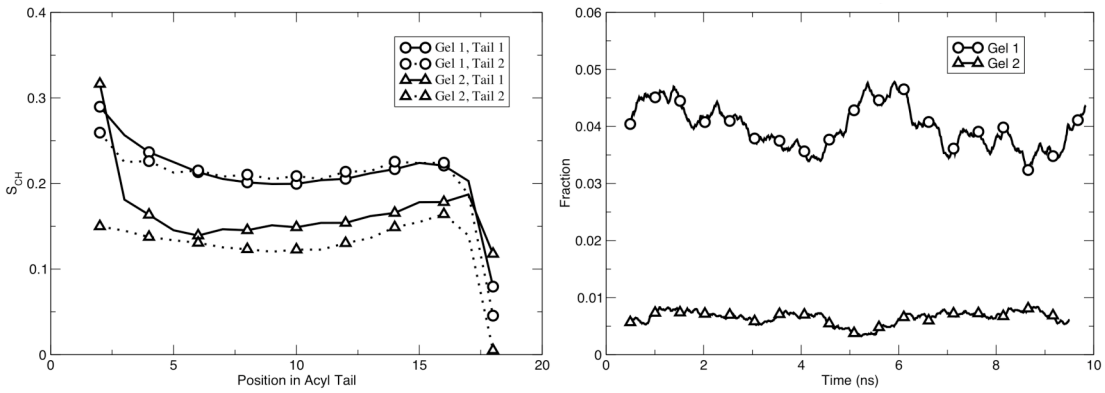

Figure 5. *Tail order.* S_{CH} of methylene carbons as a function of position in tail is shown at right. The fraction of the position-6 tail dihedrals in the *gauche* conformation is shown as a function of time at left. The top panel shouldn't have S_{CH} for carbon 18, I have to fix that, and the time in the bottom is ns mislabeled as ps.

A subtle aspect of gel structure is the rotational order of the tails.(69) Simulation distributions of γ, the angle formed by the plane described by the carbon-carbon bonds in the tail with the plane described by the tail-tilt direction and the bilayer normal (fig. 2, bottom left) show a peak at $\gamma = 90°$ for both BD and BO gels, which is consistent with a report by Nagle, et al.(69) Furthermore, rotational order g given by

$$g = \left\langle 2\cos^2\gamma - 1 \right\rangle \qquad \text{Equation 4}$$

is an order parameter to describe the breadth of the γ distribution, with more negative values indicating stronger ordering. Values of g determined for simulated BO and BD structures of DSPC at 313 K, -0.28 and -0.20 respectively, are both comparable to g = 0.26 determined experimentally for DPPC at 302 K. The differences in temperature make it difficult to assess which model is in better agreement with experiment with regard to this detail.

4.3.2 *Comparison with previous simulation studies*

The effects of backbone orientation being so significant, it is worth revisiting simulation studies of gels in the literature that have used ordered structures. These studies have all used all-atom versions of the CHARMM forcefield; one might expect that the explicit inclusion of tail protons would lead to a more realistic representation of tail packing. Some of these have yielded tilt angles and areas per lipid in agreement with experiment by construction, as their area was fixed at experimental values or subject to a surface tension to keep in near experimental values. (73) (18) An early, very detailed simulation study of the DPPC gel phase by Tu *et al*, although employing a fully flexible simulation box, was initiated at the experimental area per lipid and simulated for 1070 ps. While many points of agreement with experiment were established, the tilt direction was towards next-nearest neighbors ($\phi = 30°$), which is uncharacteristic of a PC gel at full hydration. (33)

The most dramatic difference arising from the choice of glycerol backbone orientation is not a structural one but one that relates to the thermodynamics of mixing within the gel phase. In a previous study, we used a semigrand canonical ensemble simulation method to model DSPC-DMPC mixtures in the fluid and gel phases over a range of differences in chemical potential $\Delta\mu$.(51) For a two-phase, two-component system at equilibrium, the chemical potential μ of each component is the same in both systems; therefore, the difference $\Delta\mu = \mu_{DMPC} - \mu_{DSPC}$ must also be equal in the gel and fluid phases at equilibrium. Without the ability to independently determine μ_{DSPC} and μ_{DMPC} we are unable to solve for the exact compositions of the two phases at coexistence, but by using

a disordered gel we were able generate a set of matched pairs ($x_{DSPC,gel}$; $x_{DSPC,fluid}$) over a range of $\Delta\mu$ that were in reasonable agreement with those seen in experiment (fig. 6, top),(45) where, for instance, at 313 K a gel phase containing ~10% DMPC/90% DSPC coexists with a fluid phase containing ~70% DMPC/30% DSPC. Repeating these simulations with the BO gel model leads exclusively to coexisting phases of nearly pure DSPC in the gel phase and nearly pure DMPC in the fluid phase. Further elevation of $\Delta\mu$ led to the melting of the gel phase, indicating the gel phase containing non-negligible amounts of the shorter tail component is unstable (fig. 6, bottom). While phase transition temperatures of the simulation model are somewhat shifted relative to experiment, there is no temperature within experimentally determined phase diagrams for DSPC/DMPC mixtures where nearly pure DSPC gel coexists with nearly pure DMPC fluid. To summarize, the ordered gel phase yields a phase diagram with a much broader coexistence region than observed in experiment, as its stability is apparently incompatible with the presence of a high fraction of shorter-tail lipid.

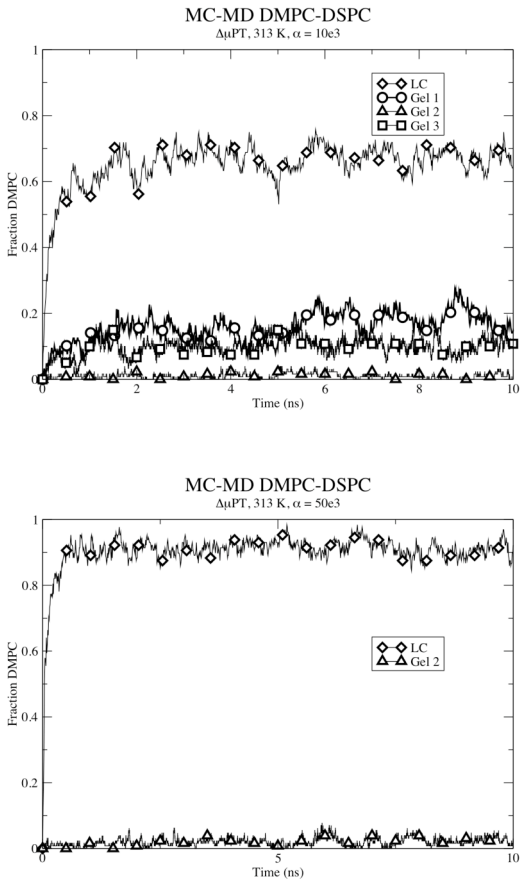

Figure 6. *Two-Component Phase Coexistence.* Lipid composition of mixed-lipid systems at a constant du are shown; in panel A, 3 gels and a LC at an activity ratio which supports non-neglible amounts of both components in both phases and panel B, lipid composition of BO and LC at 5×10^4, illustrating the unrealistically large window of gel-LC coexistence at 313 K.

4.4 Conclusions

Two DSPC gel simulation models have been constructed and compared with experimental systems and previous simulations. The models differed in their glycerol backbone lateral arrangement; the arrangement most like that predicted by experiment---disordered in the lateral superlattice---was largely in better agreement with experiment in terms of structural and thermodynamic properties. Both gels had structures qualitatively consistent with experiment in areas per lipid and tail-tilt directions. On the other hand the backbone-disordered structure had a tail tilt-angle that was significantly closer to

experiment than the backbone-ordered. These structural features, it should be noted, were more sensitive to backbone configuration than to temperature (see table 2). Finally, during semi-grand canonical ensemble simulation of DSPC/DMPC mixtures, the disordered gel structure was able to accommodate DMPC much more readily than the ordered structure, in qualitatively much better agreement with experimental phase behavior of the two-component system.

While the precise nature and degree of the backbone disorder remains an open question, the combination of experimental evidence supporting this disorder and the current demonstration of how it affects other structural properties of the gel indicates that it is an important feature to include in future atomistic models of the gel phase.

References

1. Jacobson, K., E. D. Sheets, and R. Simson. 1995. REVISITING THE FLUID MOSAIC MODEL OF MEMBRANES. Science 268:1441-1442.
2. Kusumi, A., C. Nakada, K. Ritchie, K. Murase, K. Suzuki, H. Murakoshi, R. S. Kasai, J. Kondo, and T. Fujiwara. 2005. Paradigm shift of the plasma membrane concept from the two-dimensional continuum fluid to the partitioned fluid: High-speed single-molecule tracking of membrane molecules. Annual Review of Biophysics and Biomolecular Structure 34:351-U354.
3. Jacobson, K., O. G. Mouritsen, and R. G. W. Anderson. 2007. Lipid rafts: at a crossroad between cell biology and physics. Nature Cell Biology 9:7-14.
4. Israelachvili, J. N., D. J. Mitchell, and B. W. Ninham. 1977. THEORY OF SELF-ASSEMBLY OF LIPID BILAYERS AND VESICLES. Biochimica Et Biophysica Acta 470:185-201.
5. Galla, H. J., W. Hartmann, U. Theilen, and E. Sackmann. 1979. 2-DIMENSIONAL PASSIVE RANDOM-WALK IN LIPID BILAYERS AND FLUID PATHWAYS IN BIOMEMBRANES. Journal of Membrane Biology 48:215-236.
6. Cotterill, R. M. J. 1976. COMPUTER-SIMULATION OF MODEL LIPID-MEMBRANE DYNAMICS. Biochimica Et Biophysica Acta 433:264-270.
7. Scott, H. L. 1977. MONTE-CARLO STUDIES OF HYDROCARBON REGION OF LIPID BILAYERS. Biochimica Et Biophysica Acta 469:264-271.
8. Tu, K., D. J. Tobias, and M. L. Klein. 1995. Constant pressure and temperature molecular dynamics simulation of a fully hydrated liquid crystal phase dipalmitoylphosphatidylcholine bilayer. Biophysical Journal 69:2558-2562.
9. Kenneth M. Merz, J., and B. Roux. 1996. Biological Membranes: A Molecular Perspective from Computation and Experiment. Birkhauser, Boston.
10. Klauda, J. B., M. F. Roberts, A. G. Redfield, B. R. Brooks, and R. W. Pastor. 2008. Rotation of lipids in membranes: Molecular dynamics simulation, P-31 spin-lattice relaxation, and rigid-body dynamics. Biophysical Journal 94:3074-3083.
11. de Joannis, J., Y. Jiang, F. C. Yin, and J. T. Kindt. 2006. Equilibrium distributions of dipalmitoyl phosphatidylcholine and dilauroyl phosphatidylcholine in a mixed lipid bilayer: Atomistic semigrand canonical ensemble simulations. Journal of Physical Chemistry B 110:25875-25882.
12. Coppock, P. S., and J. T. Kindt. 2010. Determination of phase transition temperatures of atomistic model lipid bilayers from stripe domain growth kinetics. Journal of Physical Chemistry Submitted.
13. Koynova, R., and M. Caffrey. 1998. Phases and phase transitions of the phosphatidylcholines. Biochimica Et Biophysica Acta-Reviews on Biomembranes 1376:91-145.

14. Le Bihan, T., and M. Pezolet. 1998. Study of the structure and phase behavior of dipalmitoylphosphatidylcholine by infrared spectroscopy: characterization of the pretransition and subtransition. Chemistry and Physics of Lipids 94:13-33.
15. Tristramnagle, S., R. M. Suter, W. J. Sun, and J. F. Nagle. 1994. KINETICS OF SUBGEL FORMATION IN DPPC - X-RAY-DIFFRACTION PROVES NUCLEATION-GROWTH HYPOTHESIS. Biochimica Et Biophysica Acta-Biomembranes 1191:14-20.
16. Marrink, S. J., J. Risselada, and A. E. Mark. 2005. Simulation of gel phase formation and melting in lipid bilayers using a coarse grained model. Chemistry and Physics of Lipids 135:223-244.
17. Berendsen, H. J. C., D. Vanderspoel, and R. Vandrunen. 1995. GROMACS - A MESSAGE-PASSING PARALLEL MOLECULAR-DYNAMICS IMPLEMENTATION. Computer Physics Communications 91:43-56.
18. Lindahl, E., B. Hess, and D. van der Spoel. 2001. GROMACS 3.0: a package for molecular simulation and trajectory analysis. Journal of Molecular Modeling 7:306-317.
19. Van der Spoel, D., E. Lindahl, B. Hess, G. Groenhof, A. E. Mark, and H. J. C. Berendsen. 2005. GROMACS: Fast, flexible, and free. Journal of Computational Chemistry 26:1701-1718.
20. Berger, O., O. Edholm, and F. Jahnig. 1997. Molecular dynamics simulations of a fluid bilayer of dipalmitoylphosphatidylcholine at full hydration, constant pressure, and constant temperature. Biophysical Journal 72:2002-2013.
21. Metropolis, N., A. W. Rosenbluth, M. N. Rosenbluth, A. H. Teller, and E. Teller. 1953. EQUATION OF STATE CALCULATIONS BY FAST COMPUTING MACHINES. Journal of Chemical Physics 21:1087-1092.
22. Daan, F., and S. Berend. 2002. Understanding Molecular Simulation. Elsevier.
23. Siepmann, J. I., and D. Frenkel. 1992. CONFIGURATIONAL BIAS MONTE-CARLO - A NEW SAMPLING SCHEME FOR FLEXIBLE CHAINS. Molecular Physics 75:59-70.
24. Wang, H., J. de Joannis, Y. Jiang, J. C. Gaulding, B. Albrecht, F. Yin, K. Khanna, and J. T. Kindt. 2008. Bilayer edge and curvature effects on partitioning of lipids by tail length: Atomistic simulations. Biophysical Journal 95:2647-2657.
25. Coppock, P. S., and J. T. Kindt. 2009. Atomistic Simulations of Mixed-Lipid Bilayers in Gel and Fluid Phases. Langmuir 25:352-359.
26. Leekumjorn, S., and A. K. Sum. 2007. Molecular studies of the gel to liquid-crystalline phase transition for fully hydrated DPPC and DPPE bilayers. Biochimica Et Biophysica Acta-Biomembranes 1768:354-365.
27. Qin, S. S., Z. W. Yu, and Y. X. Yu. 2009. Structural Characterization on the Gel to Liquid-Crystal Phase Transition of Fully Hydrated DSPC and DSPE Bilayers. Journal of Physical Chemistry B 113:8114-8123.
28. Phillips, M. C., Ladbrook.Bd, and D. Chapman. 1970. MOLECULAR INTERACTIONS IN MIXED LECITHIN SYSTEMS. Biochimica Et Biophysica Acta 196:35-&.
29. Shimshic.Ej, and McConnel.Hm. 1973. LATERAL PHASE SEPARATION IN PHOSPHOLIPID MEMBRANES. Biochemistry 12:2351-2360.

30. Mabrey, S., and J. M. Sturtevant. 1976. INVESTIGATION OF PHASE-TRANSITIONS OF LIPIDS AND LIPID MIXTURES BY HIGH SENSITIVITY DIFFERENTIAL SCANNING CALORIMETRY. Proceedings of the National Academy of Sciences of the United States of America 73:3862-3866.
31. Yeung, T., and S. Grinstein. 2007. Lipid signaling and the modulation of surface charge during phagocytosis. Immunological Reviews 219:17-36.
32. Morgan, M. J., Y. S. Kim, and Z. G. Liu. 2007. Lipid rafts and oxidative stress-induced cell death. Antioxidants & Redox Signaling 9:1471-1483.
33. Haest, C. W. M., A. J. Verkleij, J. Degier, R. Scheek, Ververga.Ph, and Vandeene.Ll. 1974. EFFECT OF LIPID PHASE-TRANSITIONS ON ARCHITECTURE OF BACTERIAL-MEMBRANES. Biochimica Et Biophysica Acta 356:17-26.
34. Luxo, C., A. S. Jurado, and V. M. C. Madeira. 1998. Lipid composition changes induced by tamoxifen in a bacterial model system. Biochimica Et Biophysica Acta-Biomembranes 1369:71-84.
35. Chinnapen, D. J. F., H. Chinnapen, D. Saslowsky, and W. I. Lencer. 2007. Rafting with cholera toxin: endocytosis and trafficking from plasma membrane to ER. Fems Microbiology Letters 266:129-137.
36. Huang, C. H., and S. S. Li. 1999. Calorimetric and molecular mechanics studies of the thermotropic phase behavior of membrane phospholipids. Biochimica Et Biophysica Acta-Reviews on Biomembranes 1422:273-307.
37. Sugar, I. P., T. E. Thompson, and R. L. Biltonen. 1999. Monte Carlo simulation of two-component bilayers: DMPC/DSPC mixtures. Biophysical Journal 76:2099-2110.
38. Michonova-Alexova, E. I., and I. P. Sugar. 2001. Size distribution of gel and fluid clusters in DMPC/DSPC lipid bilayers. A Monte Carlo simulation study. Journal of Physical Chemistry B 105:10076-10083.
39. Sugar, I. P., E. Michanova-Alexova, and P. L. G. Chong. 2001. Geometrical properties of gel and fluid clusters in DMPC/DSPC bilayers: Monte Carlo simulation approach using a two-state model. Biophysical Journal 81:2425-2441.
40. Michonova-Alexova, E. I., and I. P. Sugar. 2002. Component and state separation in DMPC/DSPC lipid bilayers: A Monte Carlo simulation study. Biophysical Journal 83:1820-1833.
41. Stevens, M. J. 2005. Complementary matching in domain formation within lipid bilayers. Journal of the American Chemical Society 127:15330-15331.
42. Faller, R., and S. J. Marrink. 2004. Simulation of domain formation in DLPC-DSPC mixed bilayers. Langmuir 20:7686-7693.
43. Tu, K., D. J. Tobias, J. K. Blasie, and M. L. Klein. 1996. Molecular dynamics investigation of the structure of a fully hydrated gel-phase dipalmitoylphosphatidylcholine bilayer. Biophysical Journal 70:595-608.
44. Venable, R. M., B. R. Brooks, and R. W. Pastor. 2000. Molecular dynamics simulations of gel (L-beta I) phase lipid bilayers in constant pressure and constant surface area ensembles. Journal of Chemical Physics 112:4822-4832.
45. Snyder, R. G., K. C. Tu, M. L. Klein, R. Mendelssohn, H. L. Strauss, and W. J. Sun. 2002. Acyl chain conformation and packing in

dipalmitoylphosphatidylcholine bilayers from MD simulation and IR spectroscopy. Journal of Physical Chemistry B 106:6273-6288.
46. de Vries, A. H., S. Yefimov, A. E. Mark, and S. J. Marrink. 2005. Molecular structure of the lecithin ripple phase. Proceedings of the National Academy of Sciences of the United States of America 102:5392-5396.
47. Wohlert, J., and O. Edholm. 2006. Dynamics in atomistic simulations of phospholipid membranes: Nuclear magnetic resonance relaxation rates and lateral diffusion. Journal of Chemical Physics 125.
48. Pearson, R. H., and I. Pascher. 1979. MOLECULAR-STRUCTURE OF LECITHIN DIHYDRATE. Nature 281:499-501.
49. Halgren, T. A. 1996. Merck molecular force field .1. Basis, form, scope, parameterization, and performance of MMFF94. Journal of Computational Chemistry 17:490-519.
50. Halgren, T. A. 1996. Merck molecular force field .2. MMFF94 van der Waals and electrostatic parameters for intermolecular interactions. Journal of Computational Chemistry 17:520-552.
51. Halgren, T. A. 1996. Merck molecular force field .3. Molecular geometries and vibrational frequencies for MMFF94. Journal of Computational Chemistry 17:553-586.
52. Halgren, T. A., and R. B. Nachbar. 1996. Merck molecular force field .4. Conformational energies and geometries for MMFF94. Journal of Computational Chemistry 17:587-615.
53. Berendsen, H. J. C., J. P. M. Postma, W. F. van Gunsteren, and J. Hermans. 1981. Intermolecular Forces. Reidel, Dordrecht.
54. Smith, G. S., E. B. Sirota, C. R. Safinya, R. J. Plano, and N. A. Clark. 1990. X-RAY STRUCTURAL STUDIES OF FREELY SUSPENDED ORDERED HYDRATED DMPC MULTIMEMBRANE FILMS. Journal of Chemical Physics 92:4519-4529.
55. Berendsen, H. J. C., J. P. M. Postma, W. F. Vangunsteren, A. Dinola, and J. R. Haak. 1984. MOLECULAR-DYNAMICS WITH COUPLING TO AN EXTERNAL BATH. Journal of Chemical Physics 81:3684-3690.
56. Van Gunsteren, W. F., and H. J. C. Berendsen. 1988. A Leap-frog Algorithm for Stochastic Dynamics. Molecular Simulation 1:173 - 185.
57. Siepmann, J. I., and I. R. McDonald. 1992. MONTE-CARLO SIMULATIONS OF MIXED MONOLAYERS. Molecular Physics 75:255-259.
58. Mendelsohn, R., M. A. Davies, J. W. Brauner, H. F. Schuster, and R. A. Dluhy. 1989. QUANTITATIVE-DETERMINATION OF CONFORMATIONAL DISORDER IN THE ACYL CHAINS OF PHOSPHOLIPID-BILAYERS BY INFRARED-SPECTROSCOPY. Biochemistry 28:8934-8939.
59. Tristramnagle, S., R. Zhang, R. M. Suter, C. R. Worthington, W. J. Sun, and J. F. Nagle. 1993. MEASUREMENT OF CHAIN TILT ANGLE IN FULLY HYDRATED BILAYERS OF GEL PHASE LECITHINS. Biophysical Journal 64:1097-1109.
60. Tardieu, A., V. Luzzati, and F. C. Reman. 1973. STRUCTURE AND POLYMORPHISM OF HYDROCARBON CHAINS OF LIPIDS - STUDY OF LECITHIN-WATER PHASES. Journal of Molecular Biology 75:711-&.

61. Petrache, H. I., S. W. Dodd, and M. F. Brown. 2000. Area per lipid and acyl length distributions in fluid phosphatidylcholines determined by H-2 NMR spectroscopy. Biophysical Journal 79:3172-3192.
62. Humphrey, W., A. Dalke, and K. Schulten. 1996. VMD: Visual molecular dynamics. Journal of Molecular Graphics 14:33-&.
63. Vondreele, P. H. 1978. ESTIMATION OF LATERAL SPECIES SEPARATION FROM PHASE-TRANSITIONS IN NONIDEAL 2-DIMENSIONAL LIPID MIXTURES. Biochemistry 17:3939-3943.
64. Sankaram, M. B., and T. E. Thompson. 1992. DEUTERIUM MAGNETIC-RESONANCE STUDY OF PHASE-EQUILIBRIA AND MEMBRANE THICKNESS IN BINARY PHOSPHOLIPID MIXED BILAYERS. Biochemistry 31:8258-8268.
65. Simons, K., and E. Ikonen. 1997. Functional rafts in cell membranes. Nature 387:569-572.
66. Brown, D. A., and E. London. 1998. Structure and origin of ordered lipid domains in biological membranes. Journal of Membrane Biology 164:103-114.
67. Brown, D. A., and E. London. 2000. Structure and function of sphingolipid- and cholesterol-rich membrane rafts. Journal of Biological Chemistry 275:17221-17224.
68. Edidin, M. 2003. The state of lipid rafts: From model membranes to cells. Annual Review of Biophysics and Biomolecular Structure 32:257-283.
69. Berkowitz, M. L. 2009. Detailed molecular dynamics simulations of model biological membranes containing cholesterol. Biochimica Et Biophysica Acta-Biomembranes 1788:86-96.
70. Niemela, P. S., M. T. Hyvonen, and I. Vattulainen. 2009. Atom-scale molecular interactions in lipid raft mixtures. Biochimica Et Biophysica Acta-Biomembranes 1788:122-135.
71. Rog, T., M. Pasenkiewicz-Gierula, I. Vattulainen, and M. Karttunen. 2009. Ordering effects of cholesterol and its analogues. Biochimica Et Biophysica Acta-Biomembranes 1788:97-121.
72. Ichimori, H., T. Hata, H. Matsuki, and S. Kaneshina. 1998. Barotropic phase transitions and pressure-induced interdigitation on bilayer membranes of phospholipids with varying acyl chain lengths. Biochimica Et Biophysica Acta-Biomembranes 1414:165-174.
73. Kharakoz, D. P., and E. A. Shlyapnikova. 2000. Thermodynamics and kinetics of the early steps of solid-state nucleation in the fluid lipid bilayer. Journal of Physical Chemistry B 104:10368-10378.
74. Nagle, J. F. 1993. AREA LIPID OF BILAYERS FROM NMR. Biophysical Journal 64:1476-1481.
75. Essmann, U., L. Perera, M. L. Berkowitz, T. Darden, H. Lee, and L. G. Pedersen. 1995. A SMOOTH PARTICLE MESH EWALD METHOD. Journal of Chemical Physics 103:8577-8593.
76. Allen, M. P., and D. J. Tildesley. 1987. Computer Simulation of Liquids. Oxford University Press, New York.
77. Luzzati, V., Gulikkrz.T, and A. Tardieu. 1968. POLYMORPHISM OF LECITHINS. Nature 218:1031-&.

78. Ranck, J. L., L. Mateu, D. M. Sadler, A. Tardieu, Gulikkrz.T, and V. Luzzati. 1974. ORDER-DISORDER CONFORMATIONAL TRANSITIONS OF HYDROCARBON CHAINS OF LIPIDS. Journal of Molecular Biology 85:249-&.
79. Hui, S. W. 1976. TILTING OF HYDROCARBON CHAINS IN A SINGLE BILAYER OF PHOSPHOLIPID. Chemistry and Physics of Lipids 16:9-18.
80. McIntosh, T. J. 1980. DIFFERENCES IN HYDROCARBON CHAIN TILT BETWEEN HYDRATED PHOSPHATIDYLETHANOLAMINE AND PHOSPHATIDYLCHOLINE BILAYERS - MOLECULAR PACKING MODEL. Biophysical Journal 29:237-245.
81. Katsaras, J., D. S. C. Yang, and R. M. Epand. 1992. FATTY-ACID CHAIN TILT ANGLES AND DIRECTIONS IN DIPALMITOYL PHOSPHATIDYLCHOLINE BILAYERS. Biophysical Journal 63:1170-1175.
82. Nagle, J. F. 1993. EVIDENCE FOR PARTIAL ROTATIONAL ORDER IN GEL PHASE DPPC. Biophysical Journal 64:1110-1112.
83. Sun, W. J., R. M. Suter, M. A. Knewtson, C. R. Worthington, S. Tristramnagle, R. Zhang, and J. F. Nagle. 1994. ORDER AND DISORDER IN FULLY HYDRATED UNORIENTED BILAYERS OF GEL PHASE DIPALMITOYLPHOSPHATIDYLCHOLINE. Physical Review E 49:4665-4676.
84. Raghunathan, V. A., and J. Katsaras. 1996. L(beta')->L(c') phase transition in phosphatidylcholine lipid bilayers: A disorder-order transition in two dimensions. Physical Review E 54:4446-4449.
85. Coppock, P. S., and J. T. Kindt. 2010. Determination of phase transition temperatures of atomistic model lipid bilayers from stripe domain growth kinetics. Journal of Physical Chemistry B Accepted.
86. Heller, H., M. Schaefer, and K. Schulten. 1993. MOLECULAR-DYNAMICS SIMULATION OF A BILAYER OF 200 LIPIDS IN THE GEL AND IN THE LIQUID-CRYSTAL PHASES. Journal of Physical Chemistry 97:8343-8360.
87. Essmann, U., L. Perera, and M. L. Berkowitz. 1995. THE ORIGIN OF THE HYDRATION INTERACTION OF LIPID BILAYERS FROM MD SIMULATION OF DIPALMITOYLPHOSPHATIDYLCHOLINE MEMBRANES IN GEL AND LIQUID-CRYSTALLINE PHASES. Langmuir 11:4519-4531.
88. Tristram-Nagle, S., Y. F. Liu, J. Legleiter, and J. F. Nagle. 2002. Structure of gel phase DMPC determined by X-ray diffraction. Biophysical Journal 83:3324-3335.
89. Wiener, M. C., R. M. Suter, and J. F. Nagle. 1989. STRUCTURE OF THE FULLY HYDRATED GEL PHASE OF DIPALMITOYLPHOSPHATIDYLCHOLINE. Biophysical Journal 55:315-325.